Biogerontology (2025) 26:202
https://doi.org/10.1007/s10522-025-10336-6

RESEARCH ARTICLE

miRNA changes with ageing and caloric restriction in male rat skeletal muscle: potential roles in muscle cell function

Gulam Altab · Brian J. Merry · Charles W. Beckett · Priyanka Raina · Ana Soriano-Arroquia · Bruce Zhang · Aphrodite Vasilaki · Katarzyna Goljanek-Whysall · João Pedro de Magalhães

Received: 12 May 2025 / Accepted: 8 October 2025 / Published online: 11 November 2025

Abstract The mechanisms underlying skeletal muscle ageing, whilst poorly understood, are thought to involve dysregulated micro (mi)RNA expression. Using young and aged rat skeletal muscle tissue, we applied high-throughput RNA sequencing to comprehensively study alterations in miRNA expression occurring with age, as well as the impact of caloric restriction (CR) on these changes. Furthermore, the function of the proteins targeted by these age- and CR-associated miRNAs was ascertained. Numerous known and novel age-associated miRNAs were identified of which CR normalised > 35% to youthful levels. Our results suggest miRNAs upregulated with age to downregulate proteins involved in muscle tissue development and metabolism, as well as longevity pathways, such as AMPK and autophagy. Furthermore, our results suggest miRNAs downregulated with age to upregulate pro-inflammatory proteins, particularly those involved in innate immunity as well as the complement and coagulation cascades. Interestingly, CR was particularly effective at normalising miRNAs upregulated with age, rescuing their associated protein-coding genes but was less effective at rescuing anti-inflammatory miRNAs downregulated with age. Lastly, the effects of a specific miRNA, miR-96-5p, identified by our analysis to be upregulated with age, were studied in cultured C2C12 myoblasts. We demonstrated miR-96-5p to decrease cell viability and markers of mitochondrial biogenesis, myogenic differentiation and autophagy. Overall, our results provide novel information regarding how miRNA expression changes in skeletal muscle, as well as the potential functional consequences of these changes and how they are ameliorated by CR.

Keywords Ageing · Caloric restriction · Non-coding RNA · miRNA · Sarcopenia · Transcriptomics

Supplementary Information The online version contains supplementary material available at https://doi.org/10.1007/s10522-025-10336-6.

G. Altab · C. W. Beckett · P. Raina · A. Soriano-Arroquia · A. Vasilaki · K. Goljanek-Whysall · J. P. de Magalhães (✉)
Integrative Genomics of Ageing Group, Institute of Ageing and Chronic Disease, University of Liverpool, Liverpool L7 8TX, UK
e-mail: jp@senescence.info

B. J. Merry
Department of Functional Genomics, Institute of Integrative Biology, University of Liverpool, Liverpool L69 7ZB, UK

A. Soriano-Arroquia
Institute of Pharmacology and Toxicology, University Hospital, University of Bonn, Bonn, Germany

B. Zhang
Institute of Healthy Ageing, and Research Department of Genetics, Evolution and Environment, University College London, London WC1E 6BT, UK

J. P. de Magalhães
Department of Inflammation and Ageing, College of Medicine and Health, University of Birmingham, Birmingham B15 2WB, UK

Introduction

Skeletal muscle ageing is associated with the progressive deterioration of muscle mass, strength and function, also known as sarcopenia (Cruz-Jentoft et al. 2019). Ageing of skeletal muscle has a profound effect on the quality of life in older individuals. The loss of muscle mass begins approximately in the 4th decade of life and continues until the end of life. Studies indicate by the time an individual reaches the age of 80, there is a reduction of 30–50% in skeletal muscle mass and function (Akima et al. 2001). Human studies have demonstrated pension-age individuals to have 30–40% less muscle strength and 25–30% less muscle size on average compared to young adults (Porter et al. 1995). The mechanisms that result in muscle ageing are not fully clear, and it is likely that numerous, interrelated processes drive the overall process. Some of the proposed mechanisms include reduced satellite cell number (Shefer et al. 2006), abnormal proteasomal degradation pathways (Fernando et al. 2019), increased ROS production (Palomero et al. 2013), mitochondrial dysfunction (Peterson et al. 2012), increased inflammation (Dalle et al. 2017) and abnormal expression long-non-coding RNAs (Marttila et al. 2020).

miRNAs are small non-coding RNAs, which negatively regulate gene expression post-translationally via mRNA repression and/or degradation. They have been identified as very important regulators in skeletal muscle proliferation and differentiation and have been demonstrated to play a role in age-related changes in skeletal muscle (Drummond et al. 2011; Wang 2013; Jung et al. 2017). Moreover, caloric restriction (CR), a widely studied method for combating ageing in animals, seems to exert its influence on skeletal muscle, in part, by attenuating age-related changes in the miRNA pool (Mercken et al. 2013; Margolis et al. 2016). With this in mind, we used rat muscle samples from a previous study (Merry et al. 2008) and isolated miRNAs to further investigate whether (1) miRNAs mediate muscle ageing, (2) CR can reverse age-associated miRNA pool changes in muscle and (3) pharmacological administration of select miRNA inhibitors/mimetics can reverse key markers of muscle ageing. We recently reported the mRNA transcriptomic landscape of these aged and caloric-restricted rats (Altab et al. 2025). Building on that work, we now present a dedicated small-RNA sequencing analysis to characterise age and CR-associated changes in miRNA expression. Given, the human suffering caused by muscle ageing and subsequent sarcopenia, this knowledge could be of huge use with regards to improving the quality of life of older adults in future.

Methods

Animals

In this study, only male Brown Norway rats were used. The rationale for this decision was to minimise biological variability associated with the oestrous cycle in females, which has been shown to influence skeletal muscle metabolism, mitochondrial function, and satellite-cell dynamics (Enns and Tiidus 2008; Enns et al. 2008). Aged mice have a considerable reduction of muscular mass in the gastrocnemius and tibialis anterior (TA) muscles (Kim et al. 2014). Thus, for this study particularly we investigated the gastrocnemius muscle. Gastrocnemius muscle tissue samples were obtained from the same cohort of rats described in a previous study (Merry et al. 2008), under Home Office Project License 40/2964. We previously published an analysis of protein-coding gene expression in this cohort (Altab et al. 2025). All animal experiments were conducted in compliance with the United Kingdom Animals (Scientific Procedures) Act of 1986.

In brief, 21–28 day old, male, Brown Norway (Substrain BN/SsNOlaHSD) rats were acquired from Harlan Laboratories, UK. Animals were kept under barrier conditions on a 12-h light:12-h dark cycle (08:00–20:00). Prior to 2 months of age, rats were group housed (n = 4) and fed ad libitum (diet procured from Special Diet Systems Division Dietex International in Witham, UK). Following maturation, all animals were moved to solitary housing and randomly assigned to either ad libitum (AL) or caloric restriction (CR) diet groups. The CR rats were fed the same diet as the ad libitum rats, but their daily intake was restricted to 55% of the age-matched ad libitum intake. The CR rats were given access to food for a limited time each day between 10:30 and 11:00 h, while the ad libitum rats had unlimited access to the food for 24 h per day. Animals were either terminated at 6 or 28 months of age (Table 1). No animals

Table 1 Group Identity, Diet Regimen and Age at Termination. Tissue samples were collected from male Brown Norway rats from one of 3 groups (n = 6). Following animal arrival at 21–28 days of age, all animals were fed ad libitum (AL). After reaching full maturation/2-months old, animals were randomly allocated to either an AL (groups 1–2) or caloric restriction (CR) diet (group 3). Half the AL-fed animals were terminated at 6-months old and half at 28-months old. CR rats were terminated at 28-months old. Tissue samples were collected immediately post-sacrifice, snap frozen and stored at -80 °C until the day of analysis

Group	Diet	Age at Termination (months)	Number of Animals
1	Ad Libitum	6	6
2	Ad Libitum	28	6
3	Caloric Restriction	28	6

displayed any signs of clinical pathology prior to sacrifice. Following termination, gastrocnemius muscle tissue was removed, flash-frozen and stored at − 80 °C, prior to further analysis.

RNA extraction and RNA-Seq analysis

Following removal from storage, gastrocnemius muscle tissues were immediately transferred onto ice to prevent thawing and degradation. Subsequently, each tissue was ground into a powder using a mortar and pestle. Liquid nitrogen was added periodically to ensure tissues remained in their frozen state. miRNA was isolated using the RNeasy Plus Universal Mini Kit (Qiagen, UK), applying a protocol optimised for small RNAs and following the manufacturer's instructions. Extracted RNA quantity and quality were assessed on a NanoDrop 2000 spectrophotometer and using the Agilent 2100 Bioanalyser, revealing all extracted RNA samples to be of high quality (RIN > 8). In addition, agarose gel electrophoresis demonstrated intact 28S and 18S rRNA bands (see Additional file: Figure S1). On average, more than 65% of reads mapped to known miRNAs (range: 51–81%), consistent with good recovery of small RNAs. Full mapping statistics for all 18 samples are provided in Additional file: Table S1.

Small-RNA libraries were prepared using the NEBNext® Small RNA Library Prep Kit for Illumina (New England Biolabs, USA) according to the manufacturer's instructions. The workflow included 3′ and 5′ adapter ligation, reverse transcription, PCR amplification, and gel-based size selection to enrich for small RNAs of approximately 22–30 nucleotides. Libraries were prepared at the Centre for Genomic Research (CGR), University of Liverpool, UK, and sequenced on an Illumina HiSeq 4000 platform. After adapter trimming, read lengths were centred at ~ 22 nucleotides (modal length 22 nt across all files; interquartile range ~ 20–23 nt), consistent with mature miRNA sequences. Raw FASTQ files were quality-checked and adapter-trimmed using Cutadapt (v1.2.1), followed by additional trimming with Sickle (v1.200) using a minimum window quality score of 20. Reads shorter than 12 nucleotides after trimming were discarded (see Additional file: Figure S2).

The miRDeep2 method, which identifies known and novel miRNAs across independent samples with 98.6–99.9% accuracy, was used to identify known and putative novel miRNA candidates (Friedländer et al. 2012). The novel miRNAs were then filtered using the following two criteria: 1) miRDeep2 score > 4. 2) significant randfold p-value (randfold refers to the likelihood that the predicted pre-miRNA sequence can fold into a stable RNA secondary structure). 3) At least two reads expressed in either young or old muscle samples. Although arbitrary, we chose a score of 4 to reduce the false positive detected miRNA.

Differential expression analysis

Differentially expressed miRNAs between young AL-fed, old AL-fed and old CR rats were identified by using the Bioconductor package "DESeq2" (version, 3.7) in R (version 4.1.0). Raw gene counts, detected by featureCount, were used as the input. DESeq2 is a well-known method, which offers statistical procedures for identifying differential expression by using negative binomial linear models for individual genes and uses the Wald test for significance analysis. The P-values from the Wald test were then adjusted using the Benjamini and Hochberg's method for controlling the false discovery rate (p-adj). Differentially expressed miRNAs were defined as those with a padj-value < = 0.05 and fold change (FC) > = 1.5.

Micro RNA TARGET identification

MultiMiR (version 1.20.0) in R was used to identify likely miRNA targets using information from several databases, including as miRanda, miRDB, PITA, TargetScan, MicroCosm, DIANA-microT, ElMMo, and PicTar (Ru et al. 2014). To narrow down miRNA targets identified by MultiMiR, only the top 40% of targets by score (an arbitrary cutoff) were classed as targets and any targets not found to be differentially expressed in our skeletal muscle ageing RNA-seq data were excluded. Though arbitrary, this tiered filtering focused our analysis toward the miRNA targets identified by MultiMiR with the greatest potential involvement in muscle ageing.

For novel miRNAs identified in this study, we applied a slightly different methodology as the MultiMiR package is limited to known miRNAs. We took advantage of the miRDB database (Wong and Wang 2015), to obtain predicted target genes for each of the novel miRNAs. While arbitrary, we chose a miRDB score cutoff of > 60 to retain targets for further analysis. This moderate threshold balanced our exploratory goal of evaluating a subset of predicted targets for each miRNA while excluding lower-confidence targets with scores below 60. The resulting target gene lists were then directly used as input for gene ontology and KEGG pathway enrichment analysis to predict the potential functions of the novel miRNAs. We also used this targetscan method to identify further unknown targets of miR-96-5p.

Target Gene Ontology and Pathway Analyses.

For the identified target genes, Gene ontology (GO) and KEGG pathways enrichment analysis was performed using ClusterProfiler (version 3.14.3), which enables visualization of functional profiles (Yu et al. 2012). Revigo (http://revigo.irb.hr) was used to remove redundant GO terms, clustering them based on semantic similarity. For this study, we performed GO biological process (GO-BP) analysis in the general level (GO level 3–8). Input gene sets were compared to the background (all expressed genes according to RNAseq) using the hypergeometric test to obtain the significant GO terms and KEGG pathways ($p < 0.05$) and the p-values corrected for false discovery rate (FDR). padj $<= 0.05$ in multiple testing, q-values are also projected for FDR control. The top 20 GO and KEGG pathways were then visualised using ggplot2 (version 3.3.5) in R.

RT-qPCR Validation of miRNAseq Data Analysis

Once RNA-seq results were obtained regarding which genes were differentially expressed, we examined 11 of these differentially expressed miRNAs using quantitative real-time PCR (RT-qPCR) on the gastrocnemius muscles of young (6-month-old), old (24-month-old) and old CR (28-month-old) rat to validate the age-related differentially expressed miRNA discovered by miRNA sequencing (miRNAseq). This was done to validate the results of our RNA-seq analysis.

Validated Primers for miRNAs were obtained from QIAGEN:

Assay Name	Catalogue Number
mmu-miR-31-5p	YP00205159
hsa-miR-96-5p	YPO0204417
rno-miR-380-3p	YPO2102544
hsa-miR-101-3p	YPO0204786
hsa-miR-122-5p	YP00205664
hsa-miR-20a-5p	YP00204292
hsa-miR-375	YP00204362
rno-miR-3576	YP02103725
hsa-miR-140-3p	YP00204304
mmu-miR-182-5p	YP00205089

Isolated total RNA was utilised to generate first-strand cDNA using miRCURY® LNA® RT Kit (Qiagen, UK, cat. 339,340), which was then subjected to qPCR using miRCURY LNA SYBR® Green PCR Kits (Qiagen, UK, cat. 339,346). We combined normalised data from samples of both young and old, as well as old CR, into a unified file. Subsequently, NormFinder (http://moma.dk/normfinder-software) was employed for analysis. Notably, mir-101a-3p emerged as one of the most consistently stable miRNAs across all samples and served as the internal control in our study. For RT-qPCR samples were calculated relative to rno-miR-101a-3p miRNA levels and group comparisons were conducted using One-Way ANOVA test followed by Newman-Keuls Multiple Comparison Test. The significance level was set to 5%.

C2C12 cell culture and transfection.

We used culture myoblast populations to investigate the role of a miRNA (rno-miR-96-5p), revealed by our RNA-seq/bioinformatic analyses to be important to both muscle ageing and responses to CR. We employed the C2C12 immortalised mouse myoblast cell line for our mechanistic experiments. This widely used model provides a reproducible and well-characterised system for studying myogenesis, mitochondrial function, and autophagy (Yaffe and Saxel 1977). Its use enabled controlled manipulation of miR-96-5p expression to investigate downstream effects on muscle cell viability and differentiation. While primary myoblasts would provide closer physiological relevance, the C2C12 line was selected due to its stability, accessibility, and extensive validation in ageing and muscle biology research.

C2C12 cells were grown in high gluose Dulbecco's Modified Eagle Medium (DMEM) supplemented with 10% foetal bovine serum (FBS) (Thermos Scientific, UK), 1% l-glutamine, and 1% penicillin/streptomycin. Once 90% confluent, the cells were grown in DMEM supplemented with 2% horse serum, 1% l-glutamine, and 1% penicillin/streptomycin, stimulating myogenic differentiation. Subsequently, using Lipofectamine 2000 (Thermos Scientific, UK), in triplicates C2C12 cells were transfected with either 50 nM of miR-96-5p, 50 nM of a mock mimetic (control), 100 nM of a miR-96-5p inhibitor or 100 nM of a scrambled inhibitor (control) (Qiagen, UK).

Assessment of the effect of miR-96-5p on cell viability and myogenic differentiation in C2C12 cells

Cell viability and differentiation were assessed in separate cell populations cultured and transfected using the method described above. After a 24 h post-transfection incubation period, cell viability was assessed using acridine orange (Sigma-Aldrich, A8097) /ethidium bromide (Sigma-Aldrich, E1510) (AO/EB) staining (Kasibhatla et al. 2006). In brief, the cell media was removed and washed twice with PBS before being stained with 500ul of a PBS solution containing 1:1000 ethidium bromide and 1:1000 acridine orange. 3 images were obtained per condition. Images of the cells were acquired using a fluorescence microscope with a total magnification of 100x, utilising the green channel for acridine orange and the red channel for ethidium bromide. Following fluorescent microscopy, the total numbers of live and dead cells were determined using ImageJ (Schneider et al. 2012). Subsequently, the ratio of live to dead cells was calculated to assess the overall viability of each cell population.

In other cell populations, after a 7-day period post-incubation, MF20 (myosin heavy chain) immunostaining was conducted to quantify the level of myoblast differentiation. In brief, cells were stained with both DAPI (Sigma-Aldrich)and MF20 antibodies (MF20-c 2ea, DSHB). 3 images were obtained per condition (Soriano-Arroquia et al. 2017). Following fluorescent microscopy, quantitative measures of myoblast differentiation, including fusion index, MyHC positive area and myotube diameter, were derived. For Fusion index, number of nuclei within MF20 positive cells (cells containing more than 2 nuclei) were counted manually, and the total nuclei was counted using image J "Analyse Particles" automated function. Fusion index was calculated by dividing the number of nuclei within multinucleated myotubes by the total number of nuclei in the entire field of view. Meanwhile, for each treatment condition, Image J also facilitated the measurement of the MyHC positive areas by adjusting threshold, this gave the measurement of the total area covered by MyHC-positive staining relative to the total area of the field of view. The MYHC staining threshold in ImageJ was set by accessing the 'Image' menu, selecting 'Adjust', and then 'Threshold'. Parameters were carefully adjusted to enhance MYHC positive staining visibility while minimizing background noise, ensuring effective isolation and highlighting of positive areas while mitigating the impact of extraneous background elements in the images. To measure the myotube diameter, firstly, the image containing myotubes was opened in ImageJ. A line selection tool was utilised to draw a straight line across the diameter of individual myotubes. The 'Analyse' menu was accessed, and 'Set Scale' was used to calibrate the image with known measurements. Subsequently, the 'Straight Line' tool was employed to measure the distance across the myotubes, and the recorded values were used to determine the myotube diameter.

Assessment of the effect of miR-96-5p on OGDH and mitochondrial biogenesis marker expression in C2C12 cells

We hypothesised miR-96-5p to directly downregulate OGDH expression and mitochondrial biogenesis downstream. Therefore, using qPCR, we investigated the expression of OGDH, two key factors involved in mitochondrial biogenesis, peroxisome proliferator-activated receptor gamma coactivator 1-alpha (PGC-1α) and mitochondrial transcription factor A (TFAM), and cytochrome c oxidase subunit I (COX I), a key mitochondrial protein. The miRCURY LNA RT Kit (Qiagen, UK) was used to synthesise cDNA using 50-100 ng of RNA, and the miRCURY LNA RT Kit (Qiagen, UK) was used to conduct qPCR in the Roche ® LightCycler® 480 according to the manufacturer's instructions. Validated primers were obtained from Qiagen, UK for the miRNAs. rno-miR-101a-3p or U6 was used as an internal control. As for the protein coding genes, the following primers were used; OGDH F: GGT GTCGTCAATCAGCCTGAGT R: ATCCAGCCA GTGCTTGATGTGC (Origene, UK); PGC1α F: GAACAAGACTATTGAGCGAACC, R: GAGTGG CTGCCTTGGGTA; COX1 F: ACTATACTACTA CTAACAGACCG, R: GGTTCTTTTTTTCCGGGA GT; 18S F: AGAAACGGCTACCACATCCA, R: CCCTCCAATGGATCCTCGTT (internal control); TFAM, F: GAGGCAAAGGATGATTCGGCTC, R: CGAATCCTATCATCTTTAGCAAGC (Liu et al. 2012; Fukaya et al. 2021; Sharma et al. 2021).

Assessment of the effect of miR-96-5p on mitochondrial function using citrate synthase assay

Proteins were extracted from C2C12 cells that were either treated with a control, miR-96-5p mimic or inhibitor for the purpose of conducting a citrate synthase assay. The MitoCheck® Citrate Synthase Activity Assay Kit from Cayman Scientific (USA) was utilized to measure the activity of citrate synthase. In the case of the ATP assay, C2C12 cells were transfected with control, miR-96-5p mimic, and inhibitors for a duration of 24 h.

Assessment of the effect of miR-96-5p on autophagy marker (LC3A, LC3B) expression in C2C12 cells using western blotting

C2C12 protein was extracted from cells using RIPA buffer (Sigma-Aldrich, UK. Cat # R0278) using the manufacturer's instructions. Following extraction, the isolated proteins were stored at -80 °C prior to analysis. Subsequently, the BCA assay was used to determine total protein concentration. Firstly, the protein standard was placed on ice while a portion of the sample was diluted to 1:10. Then, the BSA standard curve was produced using the manufacturer's recommendation. A working reagent of BCA solution was generated by mixing 50 parts of BCA Reagent A with 1 part of BCA Reagent B (50:1 ratio). In a 96-well plate (CoStar, USA), 20ul of protein standard and 20ul of sample proteins were added. Then, 180 µl of BCA working reagent was added to each well and the plate incubated at 37ºC in a dark room for 30 min. Following the incubation period, the plate was scanned using Spectro Star Nano (BMG LabTech, Germany) at a wavelength of 562 nm. The average absorbance was measured and utilised to quantify the protein concentration. Subsequently, SDS-PAGE electrophoresis was performed.

Following preparation of the polyacrylamide gels, it was carefully placed into the electrophoresis tank. Subsequently, cell protein samples and a protein ladder were loaded into their respective wells within the gel. The tank was filled with 1X Tris–Glycine SDS PAGE Buffer diluted in distilled water to facilitate the electrophoretic process. Additionally, protein loading buffer (prepared by mixing tracking dye at a 1:6 ratio) was added to the running buffer, aiding in the visualization of sample migration. The electrophoresis began at a lower voltage, typically set around 60 V initially, to allow the samples to traverse the stacking gel. Once the bromophenol dye migrated to approximately 2 mm from the bottom of the gel, indicating separation had occurred, the voltage was increased to 80 V. At this point, the running of the gel was halted.

For Western blotting, buffers were prepared for the transfer of proteins onto nitrocellulose membranes using the semi-dry transfer technique. A current was applied for transfer, followed by verification with Ponceau S staining. The membrane underwent blocking with 5% skim milk for 1 h, followed by immunoblotting utilising LC3 antibodies (Cell Signalling

Technology, cat: 2775) and multiple washes before analysis using the LICOR Cx system.

Dual-luciferase reporter and ATP assays

Target scan using the https://mirdb.org/custom.html database (Wong and Wang 2015) revealed significant alignment between the 3'UTR segment of OGDH and miR-96-5p in several species. Consequently, to confirm the interaction between miR-96-5p and OGDH, we created a luciferase reporter pmirGLO vector containing a segment either the OGDH 3'UTR, containing the purported miR-96-5p binding site (the OGDH wild-type; WT), or a mutant version of the OGDH 3'UTR devoid of the miR-96-5p binding site (OGDH Mutant; MUT). C2C12 cells were co-transfected with scRNA control or miR-96-5p mimic, together with the pmirGLO vector containing either WT or MUT OGDH 3'UTR.

Wild type ("CTTTGCTGTGCCAAGGCA") and mutated ("CTTTGCTTTGCCGGGGCA") seed sequence 3'UTR of OGDH were used (Thermos Scientific, UK). RT-PCR was used to amplify the OGDH 3'UTR and sub clone it into pmirGLO vector (Promega, UK). 5 × 10^4 C2C12 cells were seeded into 12 well plates. The next day, using Lipofectamine 2000, cells were co-transfected with control or miR-96-5p mimic and pmirGLO luciferase vector carrying either the OGDH 3'UTR wild-type or mutant gene. Dual-luciferase reporter gene assays were performed 24 h post-transfection. The level of ATP under different conditions was determined using the Mitochondrial ToxGlo™ Assay from Promega (UK), following the protocol provided by the manufacturer.

Statistical analysis of cell culture experiments

RT-qPCR data were analysed using the delta-delta Ct technique (2–Ct method) to determine relative expression levels between treatment conditions (Rao et al. 2013). The mean ± SEM of the results were plotted using Prism (5.01 edition) for Windows. To examine the difference between the groups, an unpaired two-tailed Student's t-test was conducted.. For the cell viability study, an unpaired two-tailed Student's t-test was conducted to compare the average live:dead cell ratio across treatment conditions. For the myogenic differentiation study, one-way analysis of variance, followed by Newman-Keuls Multiple Comparison test, were conducted to compare average fusion index, myotubule diameter and MyHC positive area between treatment conditions.

Likewise, all additional statistical analyses were performed using Prism (5.01 edition), with a significance level established at 5%. In the case of Western blot, citrate synthase assay, and luciferase assay, an Unpaired two-tailed t-test was employed to assess differences between the control and treatment groups.

Results

Identification of known and putative novel miRNA candidates expressed in rat skeletal muscle and their targets.

We analysed skeletal muscle of young (6-month-old) and old (28-month-old) AL-fed rats, and old CR (28-month-old CR) rat to examine the ageing process. We obtained small RNA reads derived from 18 miRNA libraries, multiplexed, and sequenced over 2 lanes of the HiSeq 4000 (2 × 150), generating an average of ~ 31 M paired end reads. After trimming, miRDeep2 detected 763 known miRNAs in rat skeletal muscle and identified 146 putative novel miRNA candidates, which showed significant randfold values and folded into the characteristic hairpin structure typical of mature miRNAs. The miRDeep2 algorithm found that several novel miRNAs shared homology in their seed sequence with existing miRNAs found in mice, suggesting a likely similarity. MultiMiR proposed numerous protein-coding genes to be the targets of the identified miRNAs.

Identification of miRNAs differentially expressed between the muscle of young and aged AL-fed rats.

We identified a total of 84 miRNAs that were significantly differentially expressed (FDR corrected padj-value ≤ 0.05, FC 1.5) in the muscle of aged rats fed AL compared to young rats fed AL. 36 miRNAs were significantly upregulated, of which 31 miRNAs were known and 5 were predicted as putative novel miRNA candidates discovered by miRDeep2. Meanwhile, 48

were significantly downregulated, of which 39 were known and 9 were newly discovered by miRDeep2. The top miRNAs exhibiting the greatest degree of upregulation (Table 2A) included rno-novel-132, rno-novel-79, rno-novel-78, and rno-novel-101 (novel) and rno-miR-31a-5p, rno-miR-122b, rno-miR-122-5p, rno-miR-122-3p, rno-miR-182, rno-miR-146a-5p and rno-miR-9b-5p (known). The top miRNAs exhibiting the greatest degree of downregulation (Table 2B) included rno-novel-70, rno-novel-84, rno-novel-88 and rno-novel-39 (novel) and rno-miR-539-5p, rno-miR-3576, rno-miR-369-5p, rno-miR-3578, rno-miR-434-3p, rno-miR-3543, rno-miR-376b-5p, rno-miR-136-5p, rno-miR-181d-5p, rno-miR-410-3p and rno-miR-181c-5p (known).

Identification of miRNAs differentially expressed between the muscle of aged CR and aged AL-fed rats.

We identified a total of 109 miRNAs that were significantly differentially expressed (FDR corrected padj-value ≤ 0.05, FC 1.5) in the muscle of aged rats fed CR compared to young rats fed AL. 49 miRNAs were significantly upregulated, of which 41 miRNAs were known and 8 were newly discovered by miRDeep2. Meanwhile, 60 were significantly downregulated, of which 53 were known and 7 were newly discovered by miRDeep2. The top 20 miRNAs exhibiting the greatest degree of upregulation (Table 3) and downregulation (Table 4) were ascertained.

Age-related miRNA changes in old skeletal muscle of rats partially reversed by caloric restriction.

Of the 84 miRNAs differentially expressed between aged rats fed AL and young rats fed AL, 34 (40.5%) were normalised to youthful expression levels in aged CR rats. Of the 36 miRNAs upregulated in the muscle of aged rats fed AL compared to young rats fed AL, 17 (47.2%) were suppressed in aged CR rats. Therefore, CR failed to suppress 19 (52.8%) of the miRNAs upregulated with ageing. Of the 48 miRNAs downregulated in the muscle of aged rats fed AL compared to young rats fed AL, 17 (35.4%) were rescued in aged CR rats. Therefore, CR failed to rescue 31 (64.6%) of the miRNAs downregulated with ageing (Fig. 1).

Functional and pathway analysis of protein-coding genes targeted by miRNA differentially expressed in aged rat muscle.

Target genes for the differentially expressed miRNAs were predicted using the MultiMiR package (miRanda, miRDB, PITA, TargetScan, MicroCosm, DIANA-microT, ElMMo, PicTar) for known miRNAs, and miRDB (score cutoff > 60) for putative novel miRNA candidates, as detailed in the Methods. The top-ranked predicted targets were then subjected to GO enrichment analysis, and results were summarised using REVIGO. Known upregulated miRNAs in old skeletal muscle targeted 175 protein-coding genes, which were enriched for 39 GO terms. Notable terms included cellular response to peptide hormone stimulus, skeletal muscle development, glycogen metabolic process, and skeletal muscle cell differentiation. REVIGO streamlined redundant terms, summarising target genes to be involved in skeletal muscle development, positive regulation of fatty acid oxidation, and fructose/hexose metabolism (Fig. 2A). Lastly, KEGG pathway analysis revealed miRNAs to target genes associated with cGMP-PKG signalling pathway, AMPK signalling pathway, Longevity regulating pathway, Insulin resistance, Adipocytokine signalling pathway and Autophagy signalling pathways (Fig. 2B).

Known downregulated miRNAs in old skeletal muscle targeted 202 protein-coding genes, which were enriched for 60 GO terms. Notable terms included wound healing, response to molecules of bacterial origin, response to lipopolysaccharide, regulation of body fluid levels and lymphocyte-mediated immunity. REVIGO streamlined redundant terms, summarising target genes to be involved in the protein activation cascade, regulation of body fluids, coagulation, drug metabolism, steroid metabolism and lymphocyte-mediated immunity, amongst others (Fig. 2C) Lastly, KEGG pathway analysis revealed miRNAs to target genes associated with complement and coagulation cascades, steroid biosynthesis and prion diseases (Fig. 2D).

Analysis of putative novel miRNAs upregulated in aged rat muscle using the miRDB database revealed

Table 2 Top 20 **A** upregulated and top 20 **B** downregulated known and putative novel miRNA candidates in old rat skeletal muscle compared with young rat skeletal muscle, ranked by padj-value. Rats were split into two groups (n = 6/group), which were terminated at either 6-months or 28-months old. Gastrocnemius muscle tissue was removed from rats terminated at either 6-months or 28-months old and RNA was extracted and sequenced. DESeq2 in R, analysing raw gene counts via negative binomial models and Wald test, identified differentially expressed miRNAs among young AL-fed and old CR rats, considering significance via adjusted p-values (padj) ≤ 0.05 and fold change (FC) ≥ 1.5 criteria. Differentially expressed miRNAs were defined as those with a padj-value < = 0.05 and fold change (FC) > = 1.5

A

miRNA	log2FoldChange	padj	BaseMean
rno-novel-132	25.96	6.34E-16	357.13
rno-novel-79	24.76	1.29E-14	151.92
rno-novel-78	22.93	1.42E-12	41.09
rno-novel-101	21.52	4.19E-11	14.89
rno-miR-31a-5p	3.60	1.40E-08	24.79
rno-miR-122b	4.47	6.26E-06	3592.29
rno-miR-122-5p	4.33	1.11E-05	7951.76
rno-miR-598-3p	1.20	0.000116064	175.95
rno-miR-140-3p	0.65	0.00023907	18,190.15
rno-miR-122-3p	4.26	0.000329713	52.70
rno-miR-182	1.16	0.000577317	1379.57
rno-miR-375-3p	2.70	0.000723014	34.72
rno-novel-47	10.86	0.000837844	190.99
rno-miR-483-3p	2.65	0.001388372	380.34
rno-miR-212-3p	1.95	0.001446286	9.45
rno-miR-129–1-3p	2.51	0.001446286	11.66
rno-miR-146a-5p	0.75	0.004345804	15,795.15
rno-miR-193b-3p	1.25	0.004507445	309.17
rno-miR-9b-5p	1.88	0.008134343	14.10
rno-miR-483-5p	1.88	0.01	279.16

B

miRNA	log2FoldChange	padj	BaseMean
rno-novel-70	−30.00	5.86E-21	108,074.10
rno-novel-84	−30.00	5.86E-21	11,186.94
rno-novel-88	−29.68	1.13E-20	3814.04
rno-novel-39	−26.67	1.15E-16	290.95
rno-novel-52	−26.14	4.41E-16	198.91
rno-novel-104	−25.72	1.07E-15	370.75
rno-novel-105	−25.29	3.20E-15	105.93
rno-novel-113	−23.56	3.04E-13	29.80
rno-novel-109	−22.90	1.46E-12	18.24
rno-miR-539-5p	−2.25	4.38E-10	29.71
rno-miR-3576	−2.25	1.14E-09	29.71
rno-miR-369-5p	−1.49	6.22E-09	85.71
rno-miR-3578	−1.49	6.22E-09	86.08
rno-miR-434-3p	−1.23	4.70E-06	1138.53
rno-miR-3543	−1.23	5.43E-06	1131.44
rno-miR-376b-5p	−1.94	2.17E-05	40.66
rno-miR-136-5p	−1.73	6.21E-05	83.56

Table 2 (continued)

B			
miRNA	log2FoldChange	padj	BaseMean
rno-miR-181d-5p	−1.09	0.000329713	818.24
rno-miR-410-3p	−1.34	0.000414971	55.58
rno-miR-181c-5p	–1.78	0.000450795	86.28

Table 3 Top 20 upregulated known and putative novel miRNA candidates in old calorically restricted (CR) rat skeletal muscle compared with young ad libitum (AL)-fed rats, ranked by padj-value. Rats were split into two groups (n = 6/group) and fed either ad libitum (AL) and terminated at 6-months old or CR and terminated at 28-months old. Gastrocnemius muscle tissue was removed from which RNA was extracted and sequenced. DESeq2 in R, analysing raw gene counts via negative binomial models and Wald test, identified differentially expressed miRNAs among young AL-fed and old CR rats, considering significance via adjusted p-values (padj) ≤ 0.05 and fold change (FC) ≥ 1.5 criteria. Differentially expressed miRNAs were defined as those with a padj-value < = 0.05 and fold change (FC) > = 1.5

miRNA	log2FoldChange	padj	BaseMean
rno-novel-100	26.65	1.60E-16	1345.95
rno-novel-145	24.69	2.28E-14	136.81
rno-novel-66	15.00	8.12E-13	3186.41
rno-novel-78	22.77	2.59E-12	34.61
rno-novel-102	21.76	2.47E-11	16.82
rno-miR-31a-5p	4.67	2.94E-09	47.76
rno-miR-598-3p	1.00	3.69E-09	151.63
rno-miR-346	3.29	8.79E-09	36.08
rno-novel-12	0.89	2.38E-06	6764.19
rno-miR-139-5p	0.89	2.81E-06	6881.72
rno-miR-129-5p	2.63	3.49E-06	126.20
rno-miR-9b-5p	3.11	5.44E-06	27.43
rno-miR-122b	3.66	1.82E-05	1986.57
rno-novel-49	6.48	1.82E-05	8.73
rno-miR-122-5p	3.54	2.81E-05	4482.47
rno-miR-9b-3p	2.29	3.01E-05	1973.45
rno-miR-9a-5p	2.29	3.02E-05	2033.49
rno-miR-129–1-3p	3.65	3.54E-05	18.52
rno-miR-9a-3p	2.72	4.19E-05	214.90
rno-miR-124-3p	2.76	5.01E-05	119.20

Table 4 Top 20 downregulated known and putative novel miRNA candidates in old calorically restricted (CR) rat skeletal muscle compared with young ad libitum (AL)-fed rats, ranked by padj-value. Rats were split into two groups (n = 6/group) and fed either ad libitum (AL) and terminated at 6-months old or CR and terminated at 28-months old. Gastrocnemius muscle tissue was removed from which RNA was extracted and sequenced. DESeq2 in R, analysing raw gene counts via negative binomial models and Wald test, identified differentially expressed miRNAs among young AL-fed and old CR rats, considering significance via adjusted p-values (padj) ≤ 0.05 and fold change (FC) ≥ 1.5 criteria. Differentially expressed miRNAs were defined as those with a padj-value < = 0.05 and fold change (FC) > = 1.5

miRNA	log2FoldChange	padj	BaseMean
rno-novel-88	-30.00	1.14E-20	3640.95
rno-novel-104	-26.81	1.47E-16	352.72
rno-novel-81	-26.37	2.78E-16	254.35
rno-novel-105	-25.07	9.38E-15	99.09
rno-novel-113	-23.38	6.81E-13	28.59
rno-novel-109	-22.71	2.75E-12	17.41
rno-miR-181c-3p	-1.39	9.06E-12	51.03
rno-miR-493-5p	-1.44	1.50E-10	121.41
rno-miR-1193-3p	-1.59	3.08E-09	46.20
rno-miR-539-5p	-1.82	0.000000042	29.85
rno-miR-3576	-1.81	0.000000109	29.90
rno-miR-181d-5p	-1.07	0.000000119	782.68
rno-miR-434-3p	-1.38	0.000000141	1049.36
rno-miR-3543	-1.38	0.000000145	1043.06
rno-miR-337-5p	-1.27	0.000000225	309.33
rno-miR-181c-5p	-1.76	0.000000326	82.41
rno-miR-329-3p	-1.53	0.000000377	105.51
rno-miR-409a-5p	-1.23	0.0000129	102.62
rno-miR-471-3p	-5.33	0.0000226	3.48
rno-miR-369-5p	-1.40	0.0000305	83.32

numerous target genes. These were found to be significantly associated with six GO terms: axonogenesis, stress-activated MAPK cascade, regulation of BMP signalling pathway, and glial cell migration (Fig. 3A). KEGG pathway analysis highlighted miRNAs to potentially target of crucial skeletal muscle pathways,

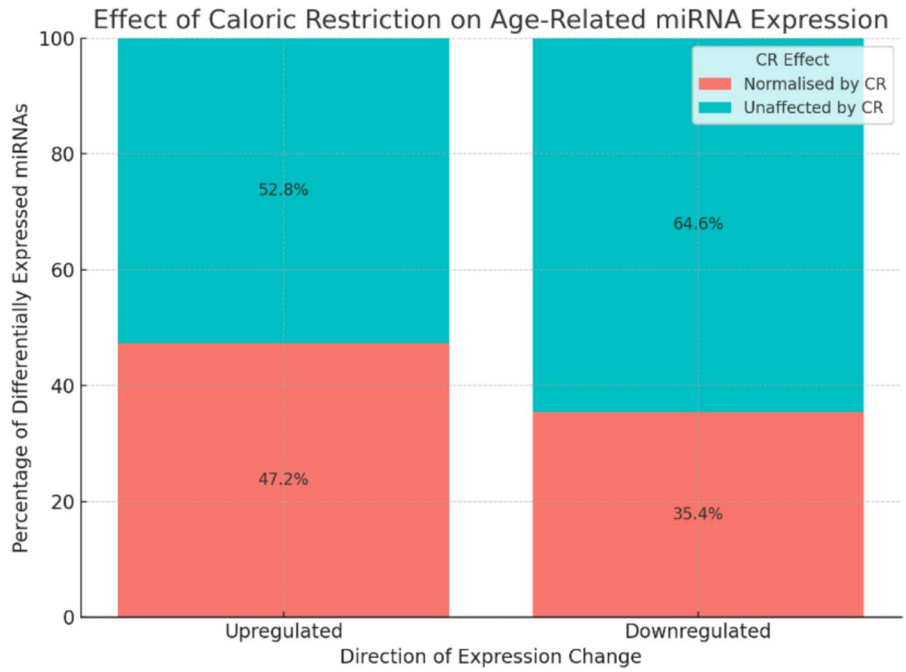

Fig. 1 Impact of CR on miRNA expression. A bar chart showing the number of genes upregulated and downregulated in the muscle of aged rats fed ad libitum (AL), when compared to the muscle of old rats fed AL, and what percentage of these are normalised by caloric restriction (CR). Upregulated miRNAs: 17 (47.2%) were normalised by CR, 19 (52.8%) were unaffected by CR; Downregulated miRNAs: 17 (35.4%) were normalised by CR, 31 (64.6%) were unaffected by CR

including PI3K-Akt, MAPK, and mTOR signalling (Fig. 3B).

Analysis of putative novel miRNAs downregulated in aged rat muscle using the miRDB database revealed numerous target genes. These were found to be significantly associated with 43 GO terms, notably including axonogenesis, angiogenesis, and forebrain development (Fig. 3C). KEGG pathway analysis for downregulated miRNAs identified 61 significantly associated pathways, notably including Proteoglycans in cancer, Axon guidance, MAPK signalling, Cellular senescence, and several other pathways (Fig. 3D).

Functional and pathway analysis of protein-coding genes targeted by miRNA uniquely differentially expressed in the muscle of aged CR rats compared to young AL-fed rats.

The miRNAs uniquely upregulated by CR were enriched for 13 GO terms. Notable terms included positive regulation of cellular carbohydrate metabolic process, positive regulation of glucose metabolic process, regulation of polysaccharide biosynthetic process and regulation of glucose metabolic process. REVIGO summarised these as related to carbohydrate metabolism and regulation of lamellipodium organisation (Fig. 4A). As for KEGG pathway analysis, we found only the ECM-receptor interaction pathway was significantly enriched, implying this pathway is downregulated in ageing of muscle under CR. It is fascinating that all the pathways that were observed in old skeletal muscle, were not enriched under CR in skeletal muscle.

The miRNAs uniquely downregulated by CR were enriched for 9 GO terms. REVIGO summarised these as involved in regulation of T cell-mediated cytotoxicity, liver development and regulation of organelle transport along microtubules (Fig. 4B). Lastly, KEGG pathway analysis revealed miRNAs to target genes associated with Allograft rejection, Graft-versus-host disease, Autoimmune thyroid disease, Type I diabetes mellitus, Cellular senescence, Viral myocarditis, Antigen processing and presentation, Epstein-Barr virus infection, Cell adhesion molecules (CAMs) amongst other pathways (Fig. 5).

RT-qPCR validation of miRNAseq data analysis

We validated differential expression of 7 miRNAs, rno-miR-122-5p, rno-miR-96-5p, rno-miR-375-5p, rno-miR-20a-5p, rno-miR-31a-5p, rno-miR-140-3p,

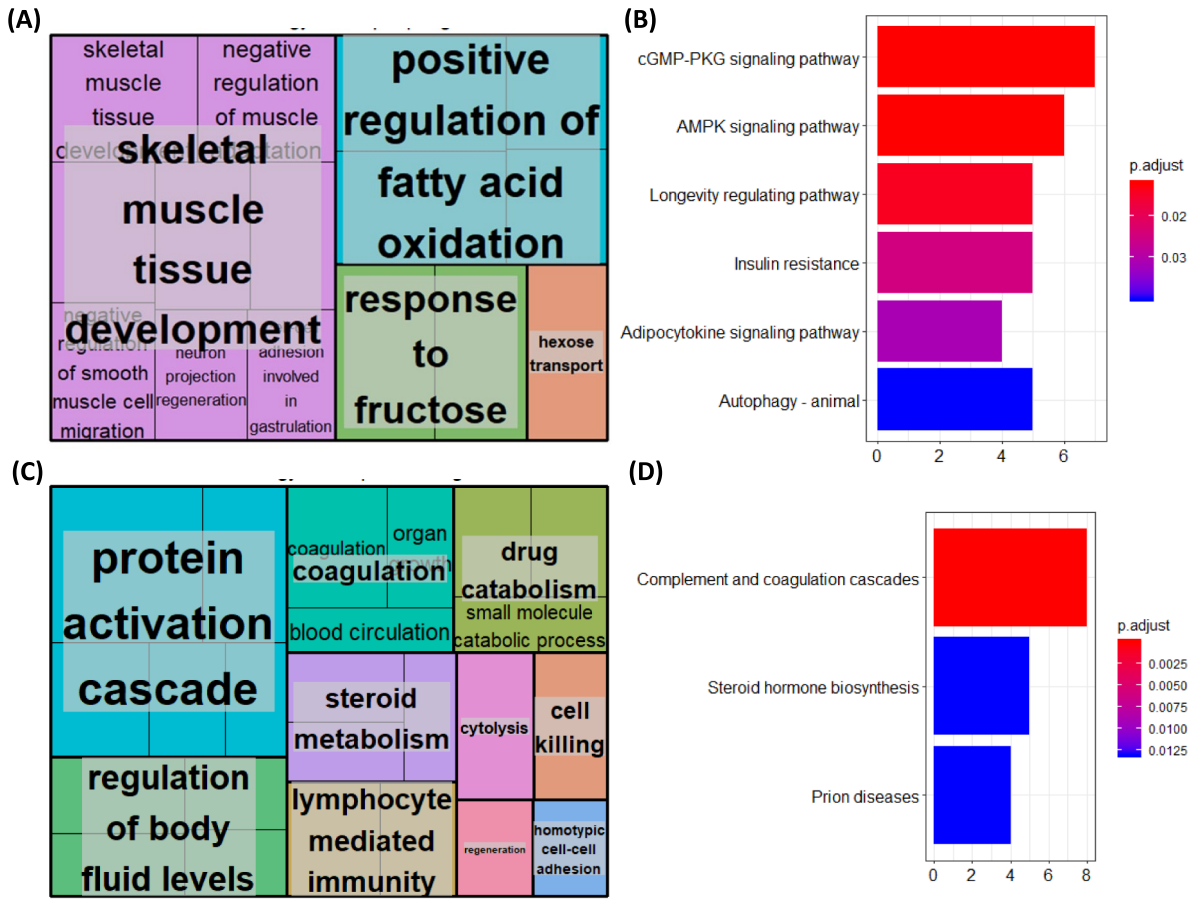

Fig. 2 Functions and pathways of genes targeted by known miRNAs upregulated **A**, **B** and downregulated **C**, **D** in the muscle of aged rats compared to young rats. Gastrocnemius muscle from 6-months or 28-months old rats was isolated and RNA extracted and sequenced. Differentially expressed miRNAs were revealed using Deseq2. For the known target genes of differentially expressed miRNAs, gene ontology (GO) terms, which were clustered based on semantic similarity **A**, **C** and KEGG pathway enrichment were derived

and rno-miR-182, using qPCR. Four out of seven of the miRNAs showed identical results with miRNAseq data analysis. These included rno-miR-122-5p, rno-miR-96-5p, rno-miR-31a-5p and rno-miR-140-3p. These miRNAs were upregulated in old rat skeletal muscle compared to young rat skeletal muscle, and expression of these miRNAs was inhibited by CR (Fig. 6 A-D, I-L).

Whilst RT-qPCR results showed the remainder of miRNAs to exhibit similar expression trends in response to ageing and CR, they did not exactly replicate RNA-seq results. For example, RT-qPCR found rno-miR-375-5p and rno-miR-20a-5p to not be significantly differentially expressed between animal groups (Fig. 6E–H). Furthermore, whilst RT-qPCR found rno-miR-182 (Fig. 6M, N) to be upregulated in the muscle of aged rats fed AL (replicating RNA-seq results), no significant difference was found between expression in young rats fed AL and old CR rats (contrary to RNA-seq results). Nevertheless, overall RT-qPCR analysis showed consistent results with miRNAseq differential analysis, thus, demonstrating the reliability of our finding.

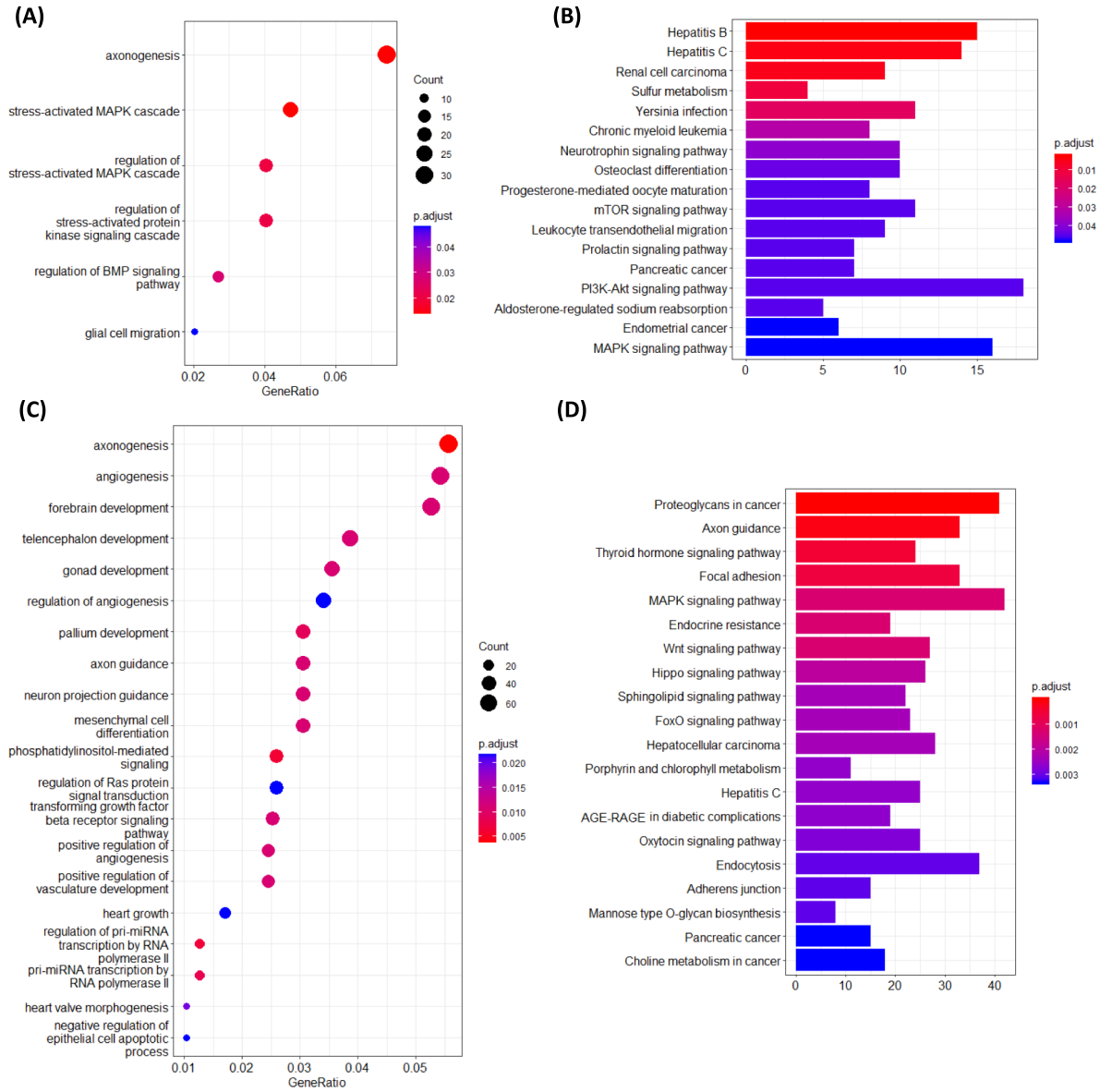

Fig. 3 Functions and pathways of genes targeted by putative novel miRNAs upregulated **A–B** and downregulated **C–D** in the muscle of aged rats compared to young rats. Gastrocnemius muscle tissue was removed from rats terminated at either 6-months or 28-months old and RNA extracted and sequenced. Differentially expressed miRNAs were revealed using Desq2. Novel miRNAs were analyzed using the mirdb.org database to predict target genes based on a cutoff score > 60, facilitating subsequent gene ontology **A**, **C**, and KEGG pathway enrichment **B**, **D** analyses to infer potential functions

Rationale for further investigating rno-miR-96-5p.

The miRNA rno- miR-96-5p has previously been shown to inhibit myogenic differentiation via suppression of Four-and-a-half LIM domains protein 1 (FHL1) gene expression. Interestingly, our RNA-seq and bioinformatic analyses highlighted differential expression of this miRNA to likely be a significant player both in the muscle ageing process and in the response to CR. Its target genes were found to be involved in several aspects of optimal skeletal muscle function, such as responses to insulin, promotion of

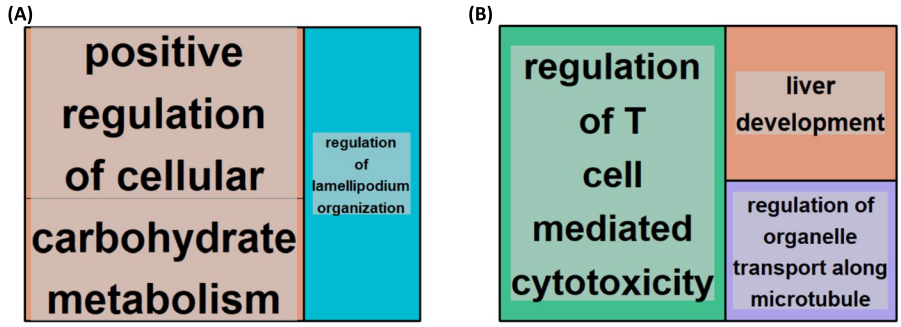

Fig. 4 Gene ontology (GO) terms associated with genes targeted by miRNAs uniquely upregulated **A** and downregulated **B** in the muscle of aged calorically restricted CR rats compared to young ad libitum (AL)-fed rats. Gastrocnemius muscle tissue was removed from rats either fed AL and terminated at 6-months or CR and terminated at 28-months old. RNA was extracted and sequenced. Differentially expressed miRNAs were revealed using Desq2 and target genes determined and associated GO terms, which were clustered based on semantic similarity **A**, **B**

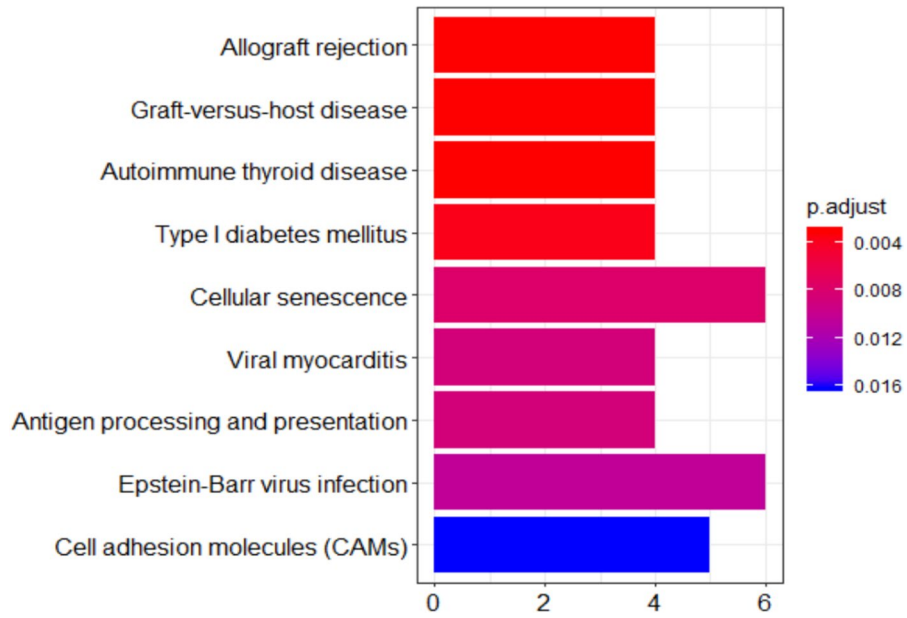

Fig. 5 KEGG pathways associated with genes targeted by miRNAs uniquely downregulated in the muscle of aged calorically restricted CR rats compared to young ad libitum (AL) rats. Gastrocnemius muscle tissue was removed from rats and RNA extracted and sequenced. KEGG pathways associated with differentially expressed miRNAs were revealed using Desq2 and ClusterProfiler

fatty acid oxidation and tissue development. Furthermore, its target genes were associated with a number of longevity-associated functions, including AMPK signalling, autophagy and responses to advanced glycation end products (AGEs). Being upregulated in aged rat muscle, rno-miR-96-5p likely plays a role in skeletal muscle dysfunction with age via downregulating many of these longevity-associated genes. We, therefore, sought to further investigate the effects of rno-miR-96-5p on myoblast function by administering a miR-96-5p mimetic and inhibitor to cultured C2C12 cells. Although miR-96-5p was not among the very top-ranked age-associated miRNAs by fold-change, it was significantly upregulated with age and reduced by CR in our dataset (Fig. 6 B, D). We therefore prioritised it for functional studies to test whether modulation of miR-96-5p could represent one pathway by which CR exerts protective effects on skeletal muscle.

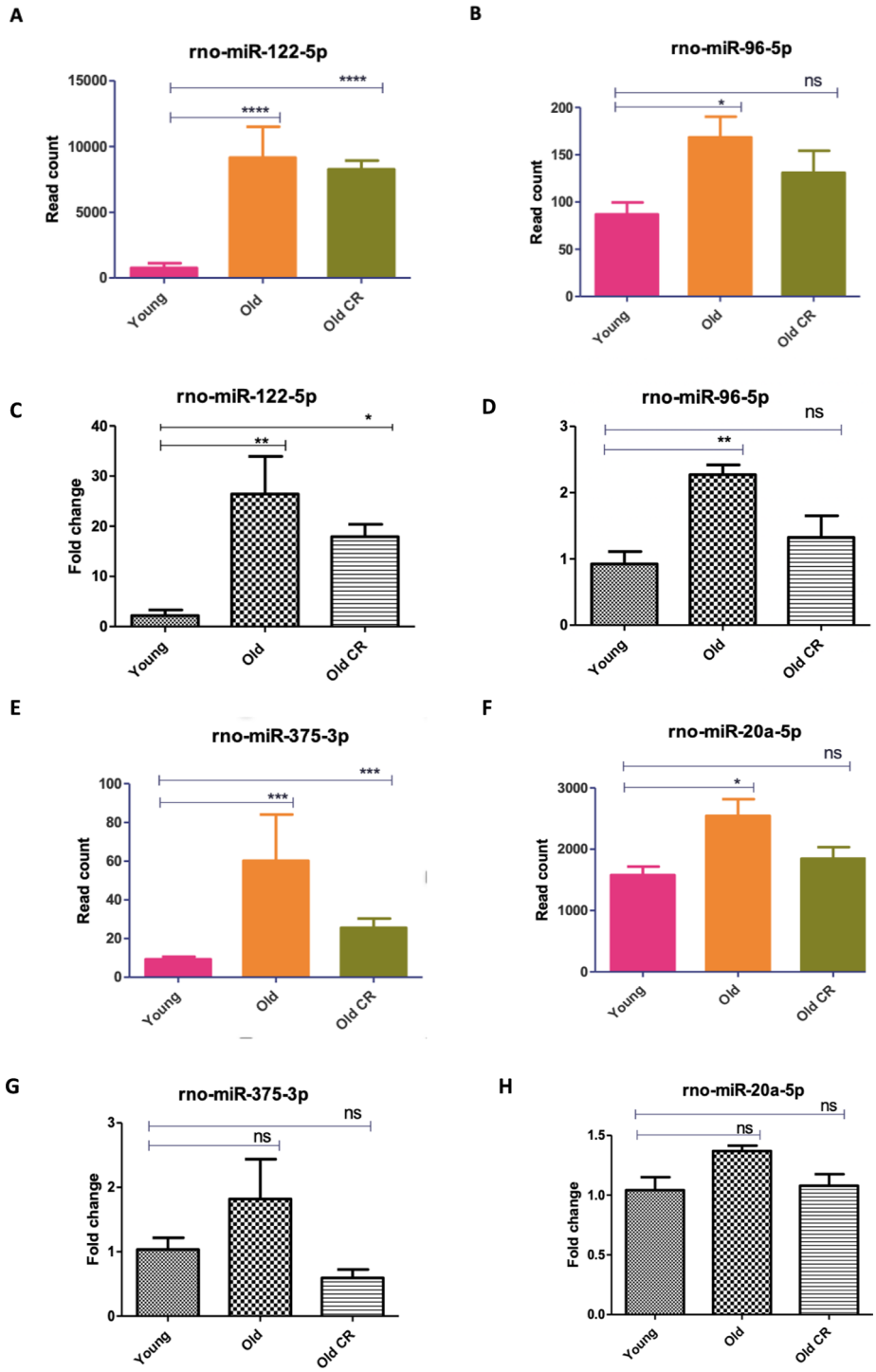

Fig. 6 RT-qPCR validation of miRNA-seq results. RNA was extracted from the gastrocnemius muscle of all rats and analysed using both RNA-seq and qPCR. For RT-qPCR samples differential expression was calculated in fold change relative to a housekeeper miRNA, rno-miR-101a-3p. Graphs showing normalised read count from microRNA-seq data. Group comparisons were conducted using One-Way ANOVA test followed by Newman-Keuls Multiple Comparison Test. (A-B,E–F,I-J, M) show miRNA-seq results and (C-D,G-H,K-L, N) show RT-qPCR results. All p-values are unadjusted for rt-qpcr. Error bars represent mean ± SEM, n = 4–6, ns denotes not significant,* = 0.01 to 0.05, ** = 0.001 to 0.01, *** = 0.0001 to 0.001 and **** = < 0.0001

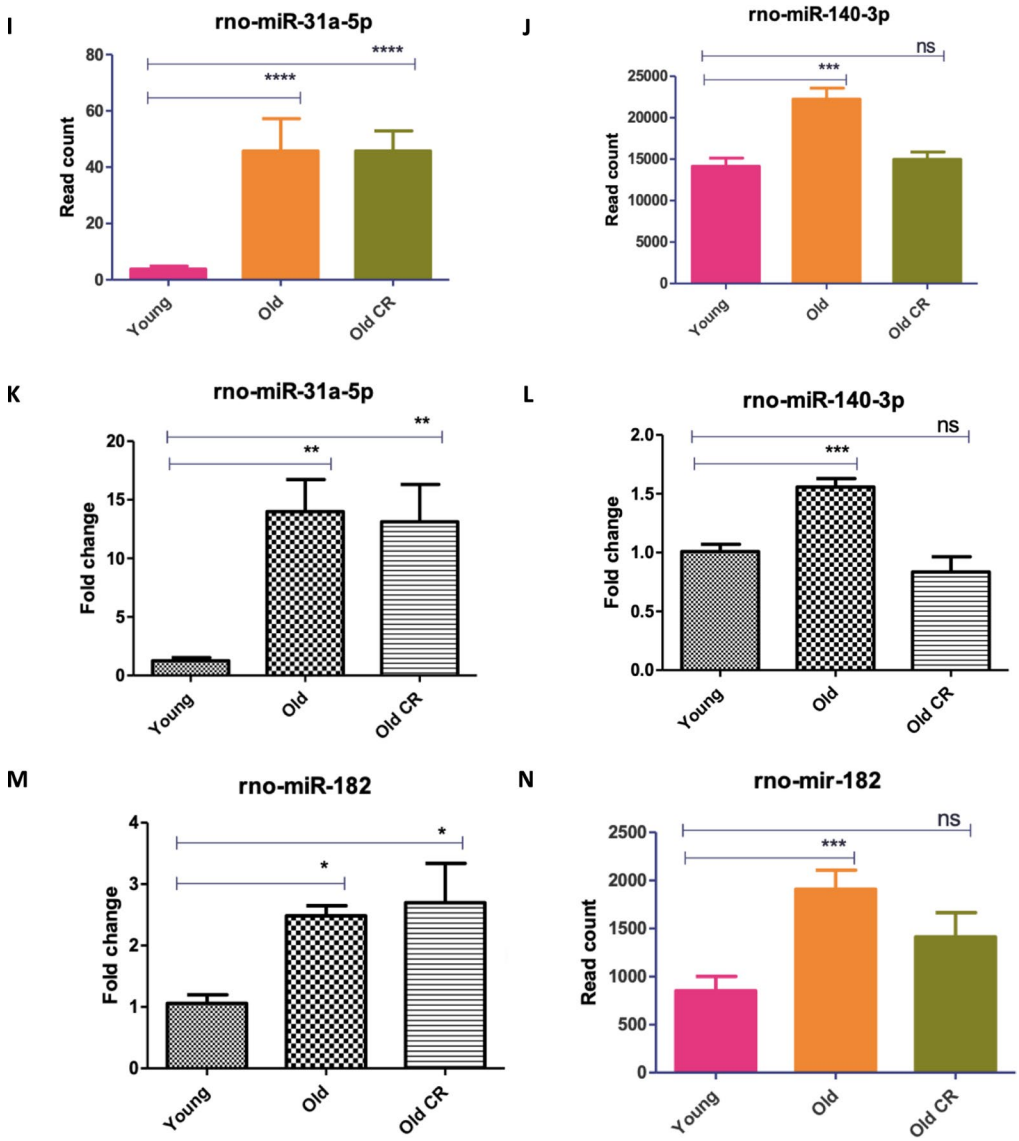

Fig. 6 (continued)

The effect of miR-96-5p on viability and myogenic differentiation in cultured C2C12 cells.

AO/EB staining revealed there to be no significant effect of 50 nM miR-96-5p on the ratio of live to dead cells compared to the population receiving 50 nM of the mock mimetic. However, the cell population transfected with 100 nM of the miR-96-5p inhibitor had a significantly higher ratio of live to dead cells compared to the population receiving 100 nM of the mock inhibitor (Fig. 7B, F).

MF20 (myosin heavy chain) immunostaining revealed the cell population transfected with 50 nM miR-96-5p to have a significantly lower fusion index, myotubule diameter and MyHC positive area compared to the cell population transfected with 50 nM of the mock mimetic indicating this miR negatively regulates myogenesis. No other significant group effects were found for any measure. However, there was a non-significant trend toward a lower MyHC positive area in cells receiving the miR-96-5p inhibitor (Fig. 7 A, C, D, E). It is possible that the effects of inhibition

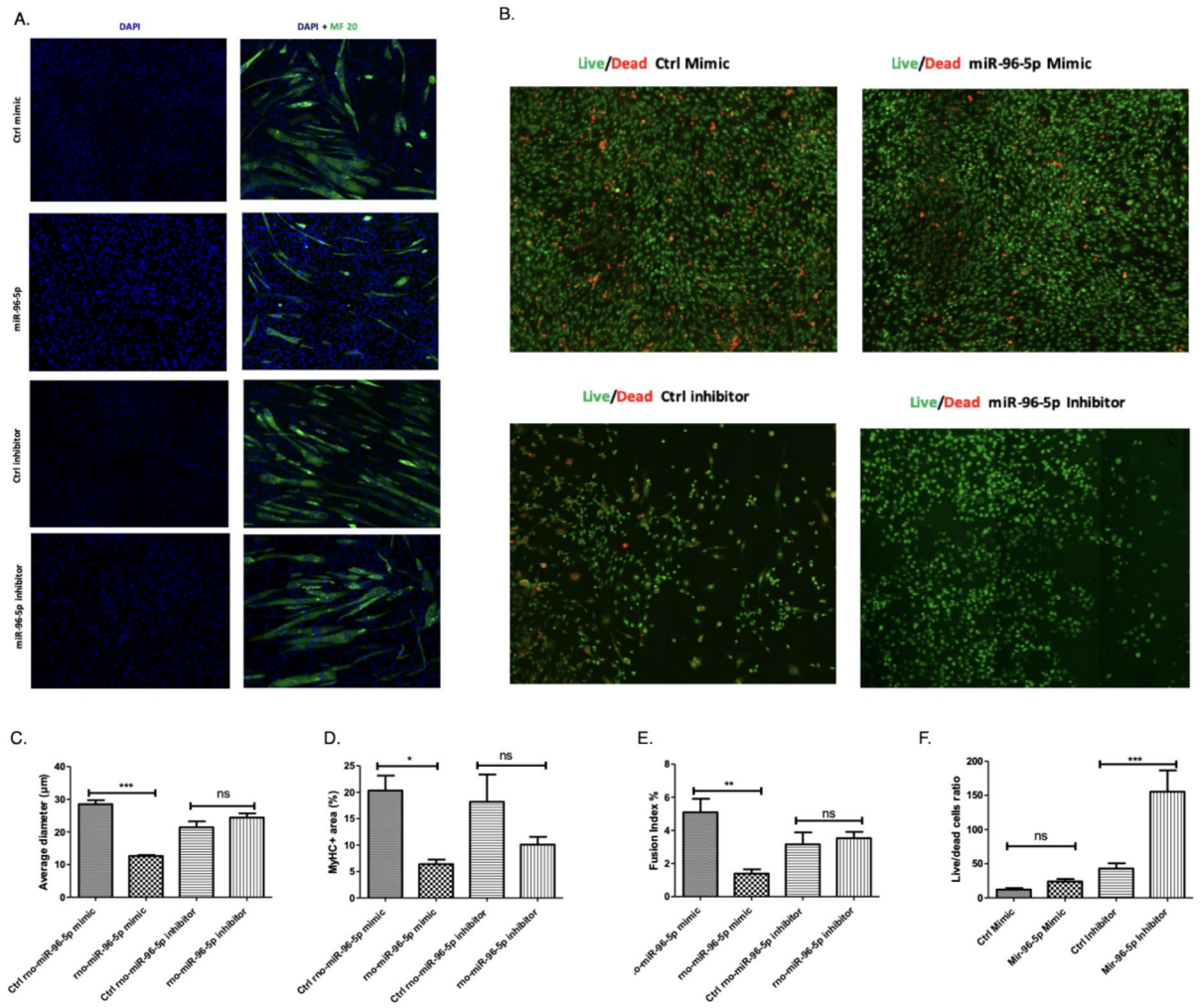

Fig. 7 Myogenic differentiation and cell viability are reduced by over-expression of miR-96-5p in C2C12 cells. C2C12 myoblasts were transfected with either 50 nM of a control mimetic, 50 nM of miR-96-5p mimetic, 100 nM of a control inhibitor or 100 nM of a miR-96-5p inhibitor. A, C–E Myoblast nuclei were stained with DAPI and heavy chain of myosin II was stained with an immunofluorescent MF20 antibody. Myotube diameter C and MyHC positive area D were ascertained using ImageJ. The fusion index E was quantified by dividing the number of multinucleated myotubes by the total number of nuclei in the entire field of view across multiple images and analysed by one-way analysis of variance and Newman-Keuls Multiple comparisons test. **B**, **F** Acridine orange/ethidium bromide revealed the number of live and dead cells in each cell population. The average live:dead cells ratio was calculated for each treatment condition and compared using unpaired two-tailed Student's t-tests. All statistical tests were conducted in Prism. Error bars represent mean ± SEM, n = 3–4, ns denotes not significant, * = 0.01 to 0.05, ** = 0.001 to 0.01, *** = 0.0001 to 0.001 and **** = p-value < 0.0001

of miR-96 may need to be explored in stress conditions to uncover a potential functional effect.

The effect of miR-96-5p on mitochondrial biogenesis markers

qPCR revealed that cells transfected with miR-96-5p to have no significantly lower expression of TFAM compared to control transfected cells. No significant differences between these groups were observed with regard to the expression of PGC-1α or COX I. Cells transfected with the miR-96-5p inhibitor displayed significantly higher expression levels of PGC-1α, COX I and TFAM compared to cells receiving the mock inhibitor (Fig. 8A).

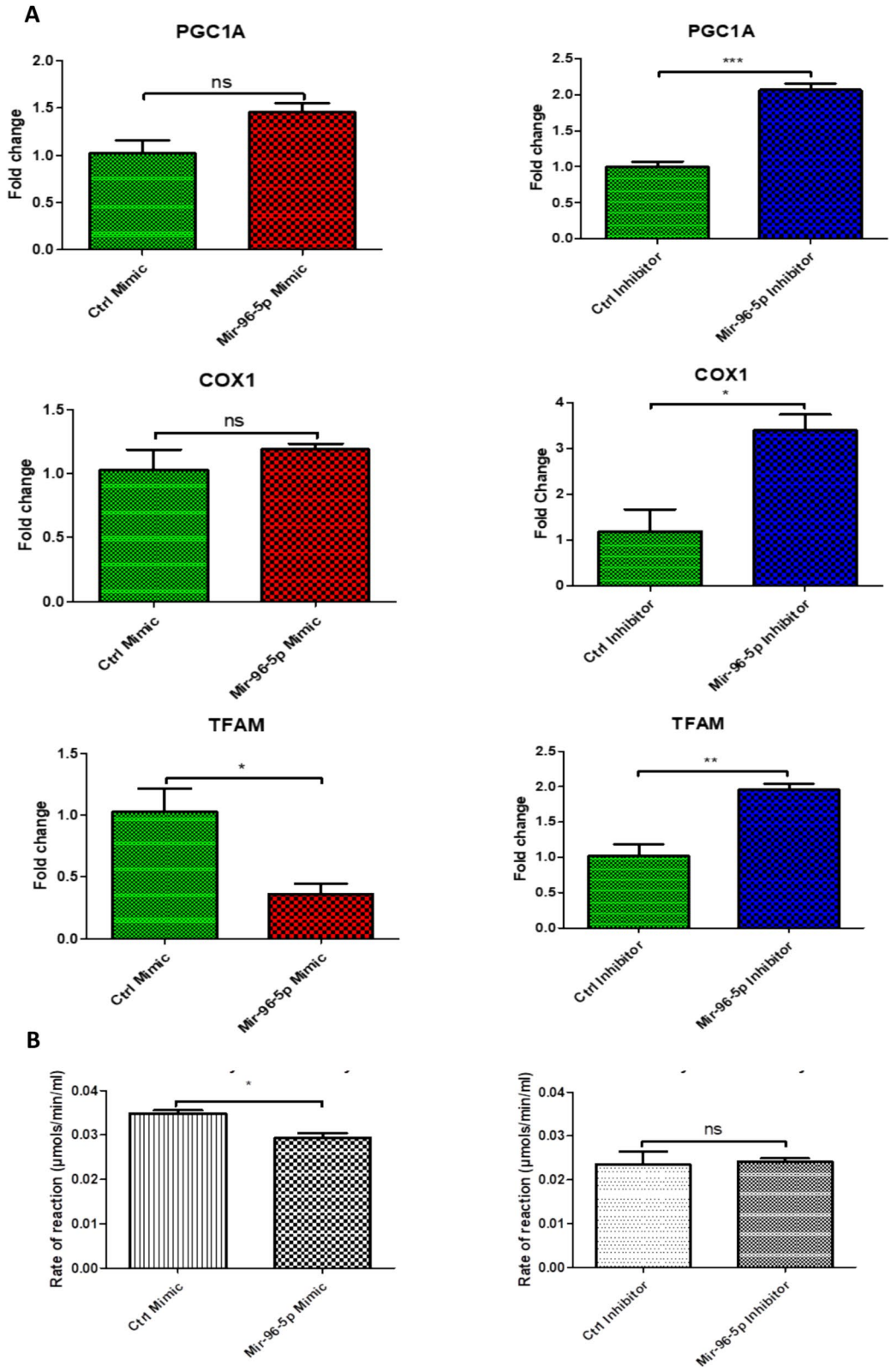
A
PGC1A
Fold change
ns
Ctrl Mimic
Mir-96-5p Mimic
PGC1A
***
Ctrl Inhibitor
Mir-96-5p Inhibitor
COX1
ns
COX1
*
TFAM
*
TFAM
**
B
Rate of reaction (µmols/min/ml)
*
ns

◂**Fig. 8** Effect of miR-96-5p on markers of mitochondrial biogenesis. C2C12 myoblasts were transfected with 50 nM of control mimic, 50 nM miR-96-5p mimic, 100 nM control inhibitor or 100 nM of a miR-96-5p inhibitor. **A** RT-qPCR was conducted 24 h after transfection. Expression of PGC-1α, COX1 and TFAM in C2C12 was quantified relative to 18S. **B** A citrate synthase assay was conducted using MitoCheck. The average activity for each treatment condition was determined in µmols/min/ml. Error bars represent mean ± SEM, n = 3,* = p-value < 0.01 to 0.05, ** = 0.001 to 0.01, *** = 0.0001 to 0.001

To confirm our findings, we performed a citrate synthase activity assay, which is used to determine the activity of mitochondrial citrate synthase in samples. This revealed that cells transfected with miR-96-5p to have significantly lower citrate synthase activity compared to cells transfected with the control mimetic. However, no significant difference was observed between cells treated with the control inhibitor versus the miR-96-5p inhibitor (Fig. 8B).

The effect of miR-96-5p on autophagy markers

Western blot results revealed both LC3A and LC3B, extensively used as autophagy biomarkers, to be significantly downregulated in miR-96-5p transfected cells compared to control mimic transfected cells. On the other hand, there was no significant difference in miR-96-5p inhibitor-treated compared to the control-treated cells. Our results clearly indicated miR-96-5p to be associated with autophagy protein LC3A/B. Therefore, upregulation of miR-96-5p in old muscle may partly be responsible for the decline in autophagy in aged skeletal muscle (Fig. 9).

Effect of miR-96-5p on OGDH expression and function

Quantitative PCR revealed cells transfected with miR-96-5p to have significantly lower expression of OGDH compared to cells transfected with the mock mimetic. According to qPCR, the miR-96-5p inhibitor appeared to have no effect on OGDH expression (Fig. 10A).

Target scan using the https://mirdb.org/custom.html database (Wong and Wang 2015) revealed significant alignment between the 3'UTR segment of OGDH and miR-96-5p in several species. This suggested a direct interaction to be responsible for the effects of miR-96-5p on OGDH expression. We sought to confirm this using the luciferase reporter assay, which revealed cells transfected with miR-96-5p to display reduced luciferase activity compared to cells transfected with the mock mimetic. This effect was only present in cells containing the wild-type OGDH segment but not those containing the mutant OGDH segment (Fig. 10B).

Lastly, ATP assay rendered no significant effects between groups with regard to ATP production. Saying this, there was a non-significant trend towards lower ATP production in the miR-96-5p-transfected cells and higher ATP production in the miR-96-5p inhibitor-transfected cells, when compared to the mock mimetic and mock inhibitor transfected cells respectively (Fig. 10C).

Discussion

While the exact mechanisms involved in sarcopenia are complex and not fully understood, perturbed epigenetic and post-transcriptional regulation of gene expression likely plays an important role. In particular, dysregulated miRNA expression has previously been shown to be involved (Drummond et al. 2011; Jung et al. 2017). Furthermore, caloric restriction, a potent anti-ageing intervention, appears to ameliorate age-related muscular dysfunction, in part, through reducing age-related changes in the miRNA (Mercken et al. 2013; Margolis et al. 2016). Our study aimed to explore age-related miRNA expression changes in rat skeletal muscle, comparing young, old, and caloric restriction-treated old groups, to uncover how miRNA may influence muscle ageing and how caloric restriction could potentially slow down this process.

Differential analysis of miRNA between young vs old and old CR.

We identified 84 miRNAs to be differentially expressed in the gastrocnemius muscle of aged rats compared to young rats. We also found 109 miRNAs to be differentially expressed in old CR muscle compared to young rat muscle. This indicates CR to

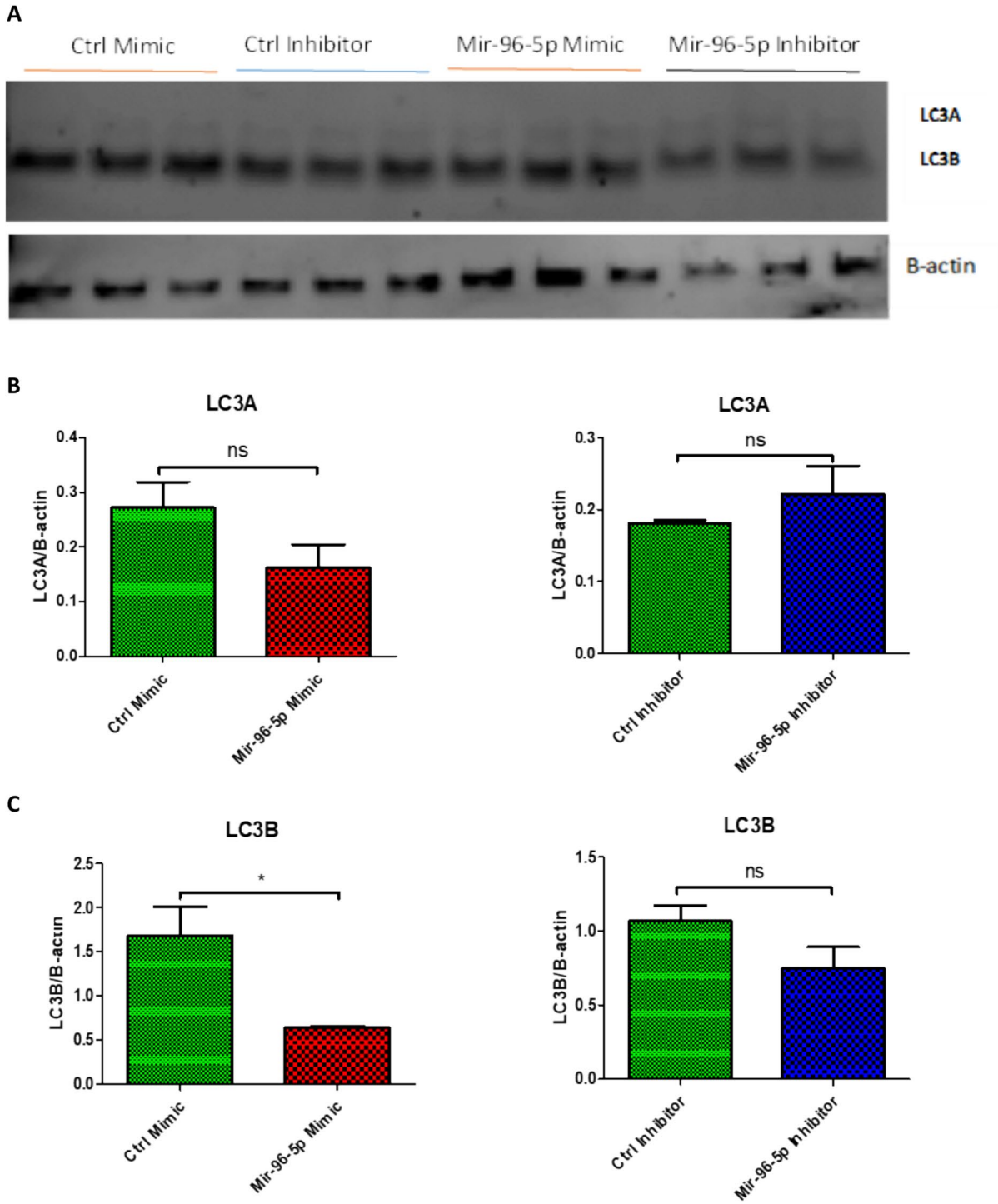

Fig. 9 MiR-96-5p reduces autophagy markers in C2C12 myoblast cells. Cells were transfected with 50 nM of control mimic, miR-96-5p mimic, or 100 nM control inhibitor or miR-96-5p inhibitor. Proteins were isolated 24 h post transfection and western blot was conducted. **A**. showing western blot image against LC3A/B upon miR-96-5p treatment, and beta actin. **B**. showing quantification of western blot for LC3A. **C**. showing quantification of western blot for LC3B. Error bars represent mean ± SEM, n = 3, ns denotes not significant, * = p-value < 0.01 to 0.05. In comparison to b-actin, the relative protein expressions were determined

have an impact on the expression of miRNAs during the processes of muscle ageing. Compared to previous studies, several of the differentially expressed miRNAs we identified have been previously reported in muscle ageing RNA-seq studies. Our analysis partially replicated findings from previous human, mouse and rhesus monkey studies. We found 4 (miR-146a-5p, miR-483-5p, miR-675-5p and miR-539-5p) and 10 (miR-434-3p, miR-181c-5p and miR-411-5p, miR-483-3p, miR-146a-5p, miR-29b-3p, miR-369-5p, miR-434-3p,miR-136-5p and miR-411-5p) miRNAs to be differentially expressed both in our study and in studies of ageing in human (Soriano-Arroquia et al. 2016) and mouse (Kim et al. 2014; Jung et al. 2017) skeletal muscle. Furthermore, our results found one (miR-495) miRNA that has previously been shown to be differentially expressed in aged Rhesus monkey skeletal muscle (Mercken et al. 2013). Where overlaps existed, several of the differentially expressed miRNAs we identified have also been highlighted in prior human, mouse, or primate studies, supporting a degree of conservation across models. At the same time, not all previously reported age- or CR-associated miRNAs were observed here, which is consistent with the variability across studies noted in the literature. Such differences are likely to reflect species- and muscle-specific effects, as well as technical differences in library preparation, sequencing depth, and bioinformatic thresholds.

GO and KEGG pathway analyses of miRNA target genes

GO analysis revealed miRNAs upregulated with age to downregulate genes involved in skeletal muscle tissue development, fatty acid oxidation regulation, and hexose metabolism, as well as cGMP-PKG AMPK, longevity regulation, insulin resistance, and pro-autophagic pathways. This suggests miRNA to be involved in age-associated impairments in muscle cell differentiation and metabolism. Furthermore, our result implicates miRNA overexpression in skeletal muscle in the downregulation of several longevity-associated processes related to insulin sensitivity, autophagy and nutrient sensing.

In addition, GO analysis revealed miRNAs downregulated with age to likely result in upregulation of genes involved in pro-inflammatory processes. Interestingly, our results suggested age-associated inflammation to result from the upregulation of complement and coagulation genes. The complement system is a proteolytic cascade that functions as a mediator of innate immunity, and the coagulation system plays a key role in haemostasis, serving as the body's first line of defence against harmful stimuli and intruders. The activation of both result in inflammatory responses, therefore, maladaptive levels of activity can lead to aberrant inflammation (Esmon 2005). This may explain the link between upregulation of complement and coagulation in aged muscle.

Lastly, GO and KEGG pathway analysis was applied to previously undiscovered miRNAs differentially expressed with age. Results of these analyses suggested these putative novel miRNA candidates to target the PI3K-Akt, MAPK, mTOR and BMP signalling. However, these remain computational predictions and require experimental validation. Many of these signalling pathways have previously been shown to be important in optimal muscle function and the ageing process. For example, both MAPK and mTOR signalling have been shown to be important in determining satellite cell fate by promoting myogenic proliferation and differentiation (Keren et al. 2006; Segalés et al. 2015; Yoon 2017). Therefore, the miRNAs discovered in this study may contribute to the age-associated depletion of the satellite cell pool (Shefer et al. 2006) and could be investigated for therapeutic potential. Notably, however, the genes purportedly targeted by these novel miRNAs were predicted based upon sequence homology. Therefore, it is crucial that both the existence and targets of these miRNAs be validated in vitro.

Impact of CR on the expression and function of differentially expressed miRNA in old skeletal muscle and their function.

Our findings are in line with a previous publication, where it was demonstrated that CR was able to reverse the expression of age-associated altered miRNAs in rhesus monkeys (Mercken et al. 2013). Specifically, we found CR to normalise the expression of more than 35% of miRNA displaying dysregulated expression with age. Interestingly, our results show CR to have had a more profound impact on upregulated miRNAs. Indeed, GO and pathway analyses

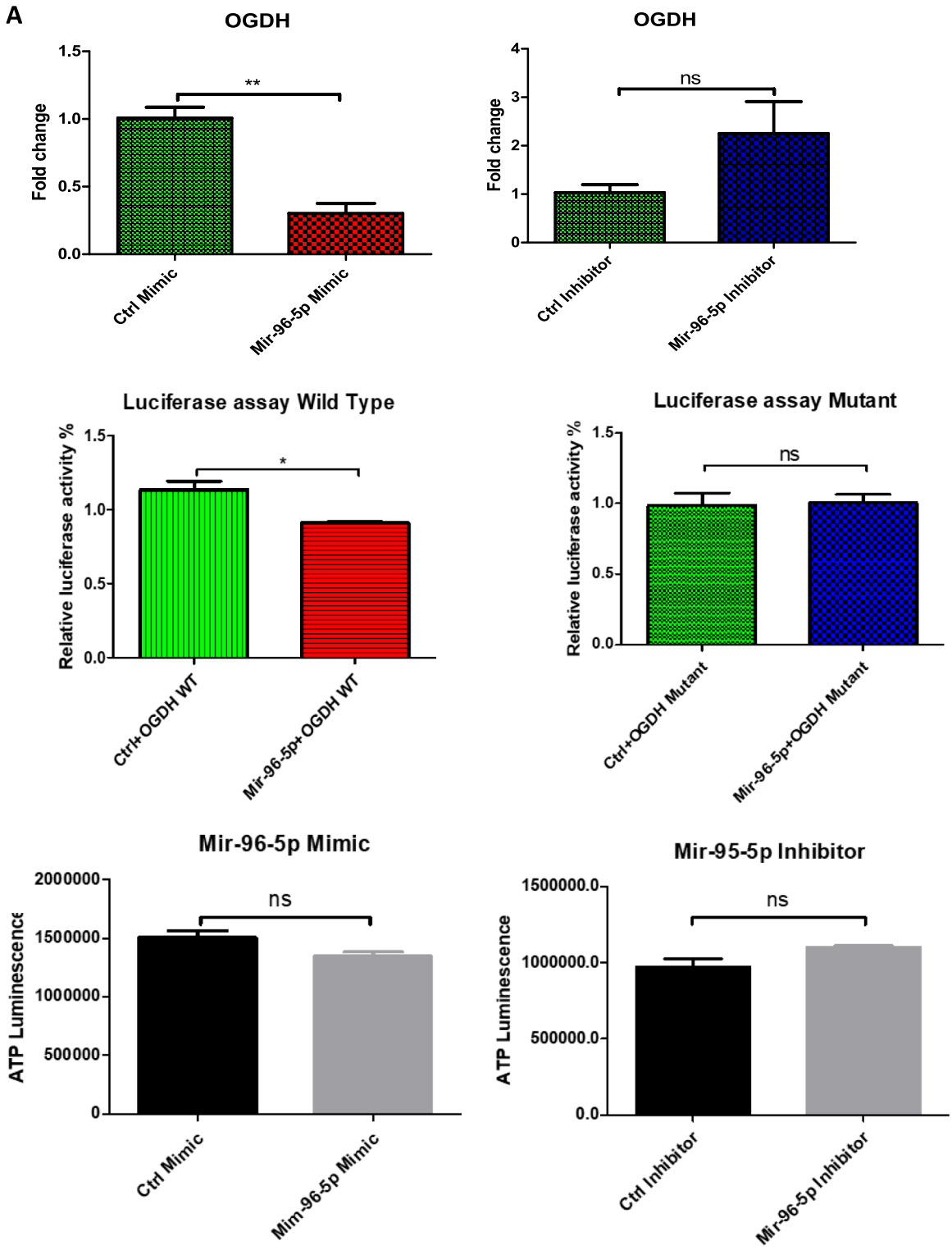
A
OGDH
Fold change
1.5
1.0
0.5
0.0
**
Ctrl Mimic
Mir-96-5p Mimic
OGDH
Fold change
4
3
2
1
0
ns
Ctrl Inhibitor
Mir-96-5p Inhibitor
B
Luciferase assay Wild Type
Relative luciferase activity %
1.5
1.0
0.5
0.0
*
Ctrl+OGDH WT
Mir-96-5p+OGDH WT
Luciferase assay Mutant
Relative luciferase activity %
1.5
1.0
0.5
0.0
ns
Ctrl+OGDH Mutant
Mir-96-5p+OGDH Mutant
C
Mir-96-5p Mimic
ATP Luminescence
2000000
1500000
1000000
500000
0
ns
Ctrl Mimic
Mim-96-5p Mimic
Mir-95-5p Inhibitor
ATP Luminescence
1500000.0
1000000.0
500000.0
0.0
ns
Ctrl Inhibitor
Mir-96-5p Inhibitor

◂**Fig. 10** Interaction between miR-96-5p and OGDH. **A** Luciferase assay, using scRNA control or miR-96-5p co-transfected in pmirGLO vector with 3'UTR segment of OGDH of wild-type (WT) or Mutant nucleotides. Cells were analysed after 24 h of transfection with 1 µg of WT or mutant plasmid and 100 nM of scRNA control or miR-96-5p mimic for luciferase activity using the Dual-Glo luciferase assay system and a luminometer. Fruit fly luciferase activity was normalised against renilla activity. **B** RT-qPCR analysis regarding the relative expression of OGDH for each treatment condition. **C** Mitochondrial ToxGlo assay was used to determine cellular ATP levels in cells treated with miR-96-5p mimic relative to the control mimic. Error bars represent mean ± SEM, n = 3, ns denotes not significant, * = p-value < 0.01 to 0.05

found the age-associated miRNAs, which CR suppressed towards youthful levels, to target many of the biological processes discussed earlier, such as those associated with skeletal muscle tissue development, metabolism and nutrient partitioning. Furthermore, through the suppression of miRNAs, CR seemed to upregulate longevity-associated AMPK and autophagy pathways (Ge et al. 2022). Notably, however, after FDR correction, the significance of the correlation between CR-suppressed miRNAs and these pathways was not maintained.

Turning to genes targeted by distinctively elevated miRNAs in response to CR, GO and KEGG pathway analyses found these to be largely associated with glucose metabolism. Reduced calorie intake is anticipated to cause a metabolic switch from carbohydrate to fatty acid oxidation (Bruss et al. 2010), therefore, this finding may be a mere artefact of this process. However, impaired glucose homeostasis (often leading to type 2 diabetes) is a well-characterised outcome of ageing (Kalyani and Egan 2013). Therefore, the miRNAs discovered to be upregulated by CR in this study may be important in understanding this symptom of ageing.

Age-associated overexpression of MiR-96-5p negatively regulates differentiation, mitochondrial biogenesis, and autophagy.

Based on bioinformatics and target analysis, we discovered that miR-96-5p is a key player in muscle ageing and a key mechanism in CR. This miRNA's target genes were linked to biological processes such as insulin responses, positive regulation of fatty acid oxidation and skeletal muscle tissue development, as well as several longevity-associated pathways. Our results demonstrated miR-96-5p inhibition to significantly increase cell viability and markers of mitochondrial biogenesis (PGC-1α, COX I and TFAM) whilst miR-96-5p activity to significantly decrease markers of myogenic differentiation and autophagy, as well as TFAM expression. This was consistent with previous findings regarding the role of miR-96-5p in the negative regulation of myogenic differentiation (Nguyen et al. 2020). In addition, we demonstrated using the luciferase reporter assay, that miR-96-5p likely directly binds to the 3'UTR of OGDH and negatively regulates its expression. In addition, we postulated that overexpression of miR-96-5p would reduce ATP synthesis due to this suppression of OGDH expression. Although there was no significant difference, we observed there was a trend of reduced ATP production for cells treated with miR-96-5p mimic, and there was a trend of upregulation in ATP production in miR-96-5p inhibitor treatment group.

Even though our findings are intriguing, many questions remain unanswered, such as how miR-96-5p regulates mitochondrial function and biogenesis. Since OGDH silencing is causally linked to a decrease in mitochondrial biogenesis and function (Nemeria et al. 2014) and miR-96-5p has no obvious binding site on PGC-1, COX1 or TFAM mRNA, it could be hypothetically attributed to the repression of OGDH mRNA by miR-96-5p. Nonetheless, during CR, we discovered that miR-95-5p expression levels were equivalent to younger muscle expression levels, and OGDH was similarly recovered. As a result, we hypothesise that these positive effects of CR are caused by CR's modulation of miRNA-96-5p in aged skeletal muscle so this should be further investigated.

Limitations

A limitation of our study is that it was restricted to male rats. Skeletal muscle ageing exhibits sexual dimorphism, with female muscle influenced by ovarian hormone status and showing distinct trajectories of decline compared with males (Enns & Tiidus 2008; De Jong et al., 2023). Moreover, oestrogen signalling has been shown to regulate both satellite cell activity and miRNA expression (Collins et al., 2019; Yoh et al., 2023). It is therefore possible that the age- and CR-associated miRNA changes we

report may differ in females. Future studies incorporating female cohorts will be required to determine whether the observed regulatory patterns are conserved across sexes.

A further limitation lies in our use of immortalised C2C12 myoblasts. While this cell line is well established and widely validated in skeletal muscle and ageing research, it does not fully recapitulate the complexity of primary myofibres, aged muscle environments, or the influence of systemic factors. Thus, future studies should ideally involve primary myoblasts from young and aged animals or in vivo models to enhance translational relevance.

A further limitation of this study is that the putative novel miRNA candidates predicted by miRDeep2 were not experimentally validated. It is therefore possible that some represent degradation fragments or alignment artefacts rather than true miRNAs. These results should thus be interpreted cautiously until validated in future studies.

Conclusion

Our study revealed previously known and unidentified miRNAs to be differentially expressed in the muscle of aged rats, as well as which of these were responsive to caloric restriction. Our results shed light on how miRNAs upregulated with age may contribute to satellite cell depletion, impaired myogenic differentiation, and metabolic dysfunction. These results were largely confirmed in our assessment of the effects of miR-96-5p in vitro. Furthermore, miRNAs upregulated with age were found to suppress a number of pro-longevity pathways, including AMPK and autophagy.

Interestingly, we also found CR to preferentially suppress miRNAs upregulated with age more so than rescue those downregulated with age. miRNAs suppressed by CR targeted many of the pathways targeted by miRNAs upregulated with age, including skeletal muscle tissue development, metabolism and nutrient partitioning, suggesting CR to upregulate these processes. However, CR was less able to downregulate the inflammatory-associated processes, thought to be dysregulated due to miRNA downregulation with age.

Acknowledgements This study is supported by the MRC-Arthritis Research UK Centre for Integrated Research into Musculoskeletal Ageing (CIMA), funded by the Medical Research Council and Versus Arthritis (grant number: MR/R502182/1) to GA. Work in our lab is further supported by grants from LongeCity, Longevity Impetus Grants/Hevolution Foundation and the Biotechnology and Biological Sciences Research Council (BB/V010123/2). The authors acknowledge the financial support of the Biotechnology and Biology Research Council under the ERA Initiative (ERA16417) for the maintenance and production of the animal model that provided the tissue samples.

Author contributions GA and JPM conceived the original idea. GA performed all the investigations and analysis. GA authored the original work, with CWB structuring the paper. The final version of the manuscript was edited and revised by GA, CWB, JPM, KGW and ASA. The study was supervised by JPM, KGW, and AV. PR and ASA assisted with both computational and laboratory investigation. BZ assisted with laboratory investigation.

Data availability The raw data can be accessed on GEO accession GSE263296.

Declarations

Competing interests JPM is CSO of YouthBio Therapeutics, an advisor/consultant for the BOLD Longevity Growth Fund and NOVOS, and the founder of Magellan Science Ltd, a company providing consulting services in longevity science. No other authors have any competing interests.

References

Akima H, Kano Y, Enomoto Y et al (2001) Muscle function in 164 men and women aged 20???84 yr. Med Sci Sports Exerc. https://doi.org/10.1097/00005768-200102000-00008

Altab G, Merry BJ, Beckett CW et al (2025) Unravelling the transcriptomic symphony of muscle ageing: key pathways and hub genes altered by ageing and caloric restriction in rat muscle revealed by RNA sequencing. BMC Genomics 26:29. https://doi.org/10.1186/s12864-024-11051-1

Bruss MD, Khambatta CF, Ruby MA et al (2010) Calorie restriction increases fatty acid synthesis and whole body fat oxidation rates. Am J Physiol Endocrinol Metab 298:E108-116. https://doi.org/10.1152/ajpendo.00524.2009

Collins BC, Arpke RW, Larson AA et al (2019) Estrogen Regulates the Satellite Cell Compartment in Females. Cell Rep 28:368–381.e6. https://doi.org/10.1016/j.celrep.2019.06.025

Cruz-Jentoft AJ, Bahat G, Bauer J et al (2019) Sarcopenia: revised European consensus on definition and diagnosis. Age Ageing 48:16–31. https://doi.org/10.1093/ageing/afy169

Dalle S, Rossmeislova L, Koppo K (2017) The role of inflammation in age-related sarcopenia. Front Physiol 8:1045. https://doi.org/10.3389/fphys.2017.01045

Drummond MJ, McCarthy JJ, Sinha M et al (2011) Aging and microrna expression in human skeletal muscle: a microarray and bioinformatics analysis. Physiol Genomics 43:595–603. https://doi.org/10.1152/physiolgenomics.00148.2010

Enns DL, Tiidus PM (2008) Estrogen influences satellite cell activation and proliferation following downhill running in rats. J Appl Physiol 104:347–353. https://doi.org/10.1152/japplphysiol.00128.2007

Enns DL, Iqbal S, Tiidus PM (2008) Oestrogen receptors mediate oestrogen-induced increases in post-exercise rat skeletal muscle satellite cells. Acta Physiol 194:81–93. https://doi.org/10.1111/j.1748-1716.2008.01861.x

Esmon CT (2005) The interactions between inflammation and coagulation. Br J Haematol 131:417–430. https://doi.org/10.1111/j.1365-2141.2005.05753.x

Fernando R, Drescher C, Nowotny K et al (2019) Impaired proteostasis during skeletal muscle aging. Free Radic Biol Med 132:58–66. https://doi.org/10.1016/j.freeradbiomed.2018.08.037

Friedländer MR, Mackowiak SD, Li N et al (2012) Mirdeep2 accurately identifies known and hundreds of novel microrna genes in seven animal clades. Nucleic Acids Res 40:37–52. https://doi.org/10.1093/nar/gkr688

Fukaya M, Sato Y, Kondo S et al (2021) Quercetin enhances fatty acid β-oxidation by inducing lipophagy in AML12 hepatocytes. Heliyon 7:e07324. https://doi.org/10.1016/j.heliyon.2021.e07324

Ge Y, Zhou M, Chen C et al (2022) Role of AMPK mediated pathways in autophagy and aging. Biochimie 195:100–113. https://doi.org/10.1016/j.biochi.2021.11.008

de Jong JCBC, Attema BJ, van der Hoek MD et al (2023) Sex differences in skeletal muscle-aging trajectory: same processes, but with a different ranking. Geroscience 45:2367–2386. https://doi.org/10.1007/s11357-023-00750-4

Jung HJ, Lee K-P, Milholland B et al (2017) Comprehensive miRNA profiling of skeletal muscle and serum in induced and normal mouse muscle atrophy during aging. J Gerontol A Biol Sci Med Sci 72:1483–1491. https://doi.org/10.1093/gerona/glx025

Kalyani RR, Egan JM (2013) Diabetes and altered glucose metabolism with aging. Endocrinol Metab Clin North Am 42:333–347. https://doi.org/10.1016/j.ecl.2013.02.010

Kasibhatla S, Amarante-Mendes GP, Finucane D et al (2006) Acridine orange/ethidium bromide (AO/EB) staining to detect apoptosis. Cold Spring Harb Protoc 2006:pdb.prot4493. https://doi.org/10.1101/pdb.prot4493

Keren A, Tamir Y, Bengal E (2006) The p38 MAPK signaling pathway: a major regulator of skeletal muscle development. Mol Cell Endocrinol 252:224–230. https://doi.org/10.1016/j.mce.2006.03.017

Kim JY, Park Y-K, Lee K-P et al (2014) Genome-wide profiling of the microrna-mRNA regulatory network in skeletal muscle with aging. Aging (Albany NY) 6:524–544. https://doi.org/10.18632/aging.100677

Liu F-L, Chen T-L, Chen R-M (2012) Mechanisms of ketamine-induced immunosuppression. Acta Anaesthesiol Taiwan 50:172–177. https://doi.org/10.1016/j.aat.2012.12.001

Margolis LM, Rivas DA, Berrone M et al (2016) Prolonged calorie restriction downregulates skeletal muscle mTORC1 signaling independent of dietary protein intake and associated microrna expression. Front Physiol. https://doi.org/10.3389/fphys.2016.00445

Marttila S, Chatsirisupachai K, Palmer D, De Magalhães JP (2020) Ageing-associated changes in the expression of lncRNAs in human tissues reflect a transcriptional modulation in ageing pathways. Mech Ageing Dev 185:111177. https://doi.org/10.1016/j.mad.2019.111177

Mercken EM, Majounie E, Ding J et al (2013) Age-associated miRNA alterations in skeletal muscle from rhesus monkeys reversed by caloric restriction. Aging 5:692–703. https://doi.org/10.18632/aging.100598

Merry BJ, Kirk AJ, Goyns MH (2008) Dietary lipoic acid supplementation can mimic or block the effect of dietary restriction on life span. Mech Ageing Dev 129:341–348. https://doi.org/10.1016/j.mad.2008.04.004

Nemeria NS, Ambrus A, Patel H et al (2014) Human 2-oxoglutarate dehydrogenase complex E1 component forms a thiamin-derived radical by aerobic oxidation of the enamine intermediate. J Biol Chem 289:29859–29873. https://doi.org/10.1074/jbc.M114.591073

Nguyen MT, Min K-H, Lee W (2020) Mir-96-5p induced by palmitic acid suppresses the myogenic differentiation of C2C12 myoblasts by targeting FHL1. IJMS 21:9445. https://doi.org/10.3390/ijms21249445

Palomero J, Vasilaki A, Pye D et al (2013) Aging increases the oxidation of dichlorohydrofluorescein in single isolated skeletal muscle fibers at rest, but not during contractions. Am J Physiol Regul Integr Comp Physiol 305:R351-358. https://doi.org/10.1152/ajpregu.00530.2012

Peterson CM, Johannsen DL, Ravussin E (2012) Skeletal muscle mitochondria and aging: a review. J Aging Res 2012:1–20. https://doi.org/10.1155/2012/194821

Porter MM, Vandervoort AA, Lexell J (1995) Aging of human muscle: structure, function and adaptability. Scandinavian Med Sci Sports 5:129–142. https://doi.org/10.1111/j.1600-0838.1995.tb00026.x

Rao X, Huang X, Zhou Z, Lin X (2013) An improvement of the 2ˆ(-delta delta CT) method for quantitative real-time polymerase chain reaction data analysis. Biostat Bioinforma Biomath 3:71–85

Ru Y, Kechris KJ, Tabakoff B et al (2014) The multimir R package and database: integration of microrna–target interactions along with their disease and drug

associations. Nucleic Acids Res 42:e133–e133. https://doi.org/10.1093/nar/gku631
Schneider CA, Rasband WS, Eliceiri KW (2012) NIH image to ImageJ: 25 years of image analysis. Nat Methods 9:671–675. https://doi.org/10.1038/nmeth.2089
Segalés J, Perdiguero E, Muñoz-Cánoves P (2015) Epigenetic control of adult skeletal muscle stem cell functions. FEBS J 282:1571–1588. https://doi.org/10.1111/febs.13065
Sharma K, Chandra A, Hasija Y, Saini N (2021) MicroRNA-128 inhibits mitochondrial biogenesis and function via targeting PGC1α and NDUFS4. Mitochondrion 60:160–169. https://doi.org/10.1016/j.mito.2021.08.008
Shefer G, Van De Mark DP, Richardson JB, Yablonka-Reuveni Z (2006) Satellite-cell pool size does matter: defining the myogenic potency of aging skeletal muscle. Dev Biol 294:50–66. https://doi.org/10.1016/j.ydbio.2006.02.022
Soriano-Arroquia A, House L, Tregilgas L et al (2016) The functional consequences of age-related changes in microRNA expression in skeletal muscle. Biogerontology 17:641–654. https://doi.org/10.1007/s10522-016-9638-8
Soriano-Arroquia A, Clegg PD, Molloy AP, Goljanek-Whysall K (2017) Preparation and culture of myogenic precursor cells/primary myoblasts from skeletal muscle of adult and aged humans. J vis Exp: Jove 120:55047. https://doi.org/10.3791/55047
Wang XH (2013) Microrna in myogenesis and muscle atrophy. Curr Opin Clin Nutr Metab Care 16:258–266. https://doi.org/10.1097/MCO.0b013e32835f81b9
Wong N, Wang X (2015) MiRDB: an online resource for microRNA target prediction and functional annotations. Nucleic Acids Res 43:D146–D152. https://doi.org/10.1093/nar/gku1104
Yaffe D, Saxel O (1977) Serial passaging and differentiation of myogenic cells isolated from dystrophic mouse muscle. Nature 270:725–727. https://doi.org/10.1038/270725a0
Yoh K, Ikeda K, Horie K, Inoue S. (2023) Roles of Estrogen, Estrogen Receptors, and Estrogen-Related Receptors in Skeletal Muscle: Regulation of Mitochondrial Function. Int J Mol Sci 24:1853. https://doi.org/10.3390/ijms24031853
Yoon M-S (2017) Mtor as a key regulator in maintaining skeletal muscle mass. Front Physiol 8:788. https://doi.org/10.3389/fphys.2017.00788
Yu G, Wang L-G, Han Y, He Q-Y (2012) clusterProfiler: an R package for comparing biological themes among gene clusters. OMICS 16:284–287. https://doi.org/10.1089/omi.2011.0118